Pollen-based quantitative land-cover reconstruction for northern Asia covering the last 40 ka

Xianyong Cao[a*], Fang Tian[a], Furong Li[b], Marie-José Gaillard[b], Natalia Rudaya[a,c,d], Qinghai Xu[e], Ulrike Herzschuh[a,d,f*]

[a] *Alfred Wegener Institute for Polar and Marine Research, Research Unit Potsdam, Telegrafenberg A43, 14473 Potsdam, Germany*

[b] *Department of Biology and Environmental Science, Linnaeus University, Kalmar SE-39182, Sweden*

[c] *Institute of Archaeology and Ethnography, Siberian Branch, Russian Academy of Sciences, pr. Akad. Lavrentieva 17, Novosibirsk 630090, Russia*

[d] *Institute of Environmental Science and Geography, University of Potsdam, Karl-Liebknecht-Str. 24, 14476 Potsdam, Germany*

[e] *College of Resources and Environment Science, Hebei Normal University, Shijiazhuang 050024, China*

[f] *Institute of Biochemistry and Biology, University of Potsdam, Karl-Liebknecht-Str. 24, Potsdam 14476, Germany*

ABSTRACT

We collected the available relative pollen productivity estimates (PPEs) for 27 major pollen taxa from Eurasia and applied them to estimate plant abundances during the last 40 cal. ka BP (calibrated thousand years before present) using pollen counts from 203 fossil pollen records in northern Asia (north of 40 °N). These pollen records were organised into 42 site-groups, and regional mean plant abundances calculated using the REVEALS (Regional Estimates of Vegetation Abundance from Large Sites)

* Corresponding authors. Alfred Wegener Institute Helmholtz Centre for Polar and Marine Research, Research Unit Potsdam, Telegrafenberg A43, Potsdam 14473, Germany. X. Cao (xcao@itpcas.ac.cn); U. Herzschuh (Ulrike.Herzschuh@awi.de). Present address for Xianyong Cao: Key Laboratory of Alpine Ecology, CAS Center for Excellence in Tibetan Plateau Earth Sciences, Institute of Tibetan Plateau Research, Chinese Academy of Sciences, Beijing 100101, China.

model. Time-series clustering, constrained hierarchical clustering, and detrended canonical correspondence analysis were performed to investigate the regional pattern, time, and strength of vegetation changes, respectively. Reconstructed regional plant-functional type (PFT) components for each site-group are generally consistent with modern vegetation, in that vegetation changes within the regions are characterized by minor changes in the abundance of PFTs rather than by increase in new PFTs, particularly during the Holocene. We argue that pollen-based REVEALS estimates of plant abundances should be a more reliable reflection of the vegetation as pollen may overestimate the turnover, particularly when a high pollen producer invades areas dominated by low pollen producers. Comparisons with vegetation-independent climate records show that climate change is the primary factor driving land-cover changes at broad spatial and temporal scales. Vegetation changes in certain regions or periods, however, could not be explained by direct climate change, for example inland Siberia, where a sharp increase in evergreen conifer tree abundance occurred at ca. 7–8 cal. ka BP despite an unchanging climate, potentially reflecting their response to complex climate–permafrost–fire–vegetation interactions and thus a possible long-term-scale lagged climate response.

Keywords: boreal forests, China, Holocene, late Quaternary, pollen productivity, quantitative reconstruction, Siberia, vegetation

1 Introduction

High northern latitudes such as northern Asia experience above-average temperature increases in times of past and recent global warming (Serreze et al., 2000; IPCC, 2007), known as polar amplification (Miller et al., 2010). Temperature rise is expected to promote vegetation change as the vegetation composition in these areas is assumed to be controlled mainly by temperature (Li J. et al., 2017; Tian et al., 2018). However, a more complex response can occur mainly because vegetation is not linearly related to temperature change (e.g. due to resilience, stable states or time-lagged responses; Soja et al., 2007; Herzschuh et al., 2016) and/or vegetation is only indirectly limited

by temperature while other temperature-related environmental drivers such as permafrost conditions are more influential (Tchebakova et al., 2005).

Such complex relationships between temperature and vegetation may help explain several contradictory findings of recent ecological change in northern Asia. For example, simulations of vegetation change in response to a warmer and drier climate indicate that steppe should expand in the present-day forest–steppe ecotone of southern Siberia (Tchebakova et al., 2009) but, contrarily, pine forest has increased during the past 74 years, probably because the warming temperature was mediated by improved local moisture conditions (Shestakova et al., 2017). In another example, evergreen conifers, which are assumed to be more susceptible to frost damage than *Larix*, expanded their distribution by 10% during a period with cooler winters from 2001 to 2012, while the distribution of *Larix* forests decreased by 40% on the West Siberian Plain as revealed by a remote sensing study (He et al., 2017). Additionally, some field studies and dynamic vegetation models infer a rapid response of the treeline to warming in northern Siberia (e.g., Moiseev, 2002; Soja et al., 2007; Kirdyanov et al., 2012), but combined model- and field-based investigations of larch stands in north-central Siberia reveal only a densification of tree-stands, not an areal expansion (Kruse et al., 2016; Wieczorek et al., 2017).

These findings on recent vegetation dynamics that contradict a straightforward vegetation-temperature relationship may be better understood in the context of vegetation change over longer time-scales. Synthesizing multi-record pollen data is the most suitable approach to investigate quantitatively the past vegetation change at broad spatial and long temporal scales. Broad spatial scale pollen-based land-cover reconstructions have been made for Europe (e.g. Mazier et al., 2012; Nielsen et al., 2012; Trondman et al., 2015) and temperate China (Li, 2016) for the Holocene. However, vegetation change studies in northern Asia are restricted to biome reconstructions (Tarasov et al., 1998, 2000; Bigelow et al., 2003; Binney et al. 2017; Tian et al., 2018), which do not reflect compositional change. Syntheses of pure pollen percentage data are not appropriate due to differences in pollen productivity,

which may result in an overestimation of the strength of vegetation changes (Wang and Herzschuh, 2011). This might be particularly severe when strong pollen producers such as pine (Mazier et al., 2012) invade areas dominated by low pollen producers such as larch (Niemeyer et al, 2015). Marquer et al. (2014, 2017) also demonstrated the strength of pollen-based REVEALS estimates of plant abundance in studies of Holocene vegetation change and plant diversity indices in Europe. Accordingly, syntheses of quantitative plant cover derived from the application of PPEs to multiple pollen records (Trondman et al., 2015; Li, 2016) should be a better way to investigate Late Glacial and Holocene vegetation change in northern Asia.

In this study, we employ the taxonomically harmonized and temporally standardized fossil pollen datasets available from eastern continental Asia (Cao et al., 2013, 2015) and Siberia (Tian et al., 2018) covering the last 40 cal. ka BP (henceforth abbreviated to ka). We compile all the available PPEs from Eurasia and use the mean estimate for each taxon. Finally, we quantitatively reconstruct plant cover using the REVEALS model (Sugita, 2007) for 27 major taxa at 18 key time slices. We reveal the nature, strength, and timing of vegetation change in northern Asia and its regional peculiarities, and discuss the driving factors of vegetation change.

2 Data and methods

2.1. Fossil pollen data process

The fossil pollen records were obtained from the extended version of the fossil pollen dataset for eastern continental Asia containing 297 records (Cao et al., 2013, 2015) and the fossil pollen dataset for Siberia with 171 records (Tian et al., 2017). For the 468 pollen records, pollen names were harmonized into genus level for arboreal taxa while family level for herbaceous taxa, and age-depth models were re-established using the Bayesian age-depth modelling (further details are described in Cao et al., 2013). We selected 203 pollen records from lacustrine sediments (110 sites) and peat (93 sites) north of 40°N, with chronologies based on ≥3 dates and <500 year/sample temporal resolution generally, following previous studies (Mazier et al., 2012; Nielsen

et al., 2012; Fyfe et al., 2013; Trondman et al., 2015). Out of the 203 pollen records, 170 sites (83 from lakes, 87 from bogs) have original pollen counts, while in the other 33 sites only pollen percentages are available. Due to overall low site density, we decided to include these data. The pollen counts were back calculated from percentages using the terrestrial pollen sum indicated in the original publications. Detailed information (including location, data quality, chronology reliability, and data source) of the selected sites is presented in Appendices 1 and 2.

Table 1 Selected time windows.

Time window (cal a BP)	Abbreviated name
-60~100	0 ka
100~350	0.2 ka
350~700	0.5 ka
700~1200	1 ka
1700~2200	2 ka
2700~3200	3 ka
3700~4200	4 ka
4700~5200	5 ka
5700~6200	6 ka
6700~7200	7 ka
7700~8200	8 ka
8700~9200	9 ka
9700~10200	10 ka
10500~11500	11 ka
11500~12500	12 ka
13500~14500	14 ka
19000~23000	21 ka
23000~27000	25 ka
36000~44000	40 ka

We selected 18 key time slices for reconstruction (Table 1) to capture the general temporal patterns of vegetation change during the last 40 ka, i.e. 40, 25, 21, 18, 14, and 12 ka during the late Pleistocene and 1000-year resolution (i.e. 500-year time windows around each millennium, e.g. 0.7–1.2 ka, 1.7–2.2 ka, etc.) during the Holocene. For the 0 ka time slice, the ca. 150-year time window (<0.1 ka) was set to represent the modern vegetation. Since few pollen records have available samples at the 0 ka time slice, the 0.2 and 0.5 ka time slices covered a 250-year or 350-year time window (0.1~0.35 ka and 0.35~0.7 ka, respectively) to represent the recent vegetation,

following the strategy and time windows implemented for Europe (Mazier et al., 2012; Trondman et al., 2015). For the last glacial period, even broader time windows were chosen to offset the sparsely available samples (Table 1). Pollen counts of all available samples within one time window were summed up to represent the total pollen count for each time slice. In this study, we selected 27 major pollen taxa (with available PPE values) that form dominant components in both modern vegetation communities and the fossil pollen spectra and reconstruct their abundances in the past vegetation (Table 2).

Table 2 Fall speed of pollen grains (FS) and mean relative pollen productivity estimate (PPE) with standard error (SE) for the 27 selected taxa. Plant-functional type (PFT) assignment is according to previous biome reconstructions (Tarasov et al., 1998, 2000; Bigelow et al., 2003; Ni et al., 2010).

PFT	**PFT description**	**pollen type**	**FS (m/s)**	**PPE (SE)**
I	evergreen conifer tree	*Pinus*	0.031 [1]	9.629 (0.075)
I	evergreen conifer tree	*Picea*	0.056 [1]	2.546 (0.041)
I	evergreen conifer tree	*Abies*	0.120 [1]	6.875 (1.442)
II	deciduous conifer tree	*Larix*	0.126 [1]	3.642 (0.125)
III	boreal deciduous tree	*Betula*_tree *Betula*_undiff.	0.024 [1]	8.106 (0.125)
III	boreal deciduous tree	*Alnus*_tree *Alnus*_undiff.	0.021 [1]	9.856 (0.092)
III	boreal deciduous tree	*Corylus*	0.025 [2]	1.637 (0.065)
IV	temperature deciduous tree	*Quercus*	0.035 [1]	6.119 (0.050)
IV	temperature deciduous tree	*Fraxinus*	0.022 [1]	2.046 (0.105)
IV	temperature deciduous tree	*Juglans*	0.037 [3]	4.893 (0.221)
IV	temperature deciduous tree	*Carpinus*	0.042 [1]	5.908 (0.285)
IV	temperature deciduous tree	*Tilia*	0.032 [2]	1.055 (0.066)
IV	temperature deciduous tree	*Ulmus*	0.032 [2]	6.449 (0.684)
V	boreal shrub	*Betula*_shrub	0.024 [1]	1.600 (0.132)
V	boreal shrub	*Alnus*_shrub	0.021 [1]	6.420 (0.420)
V	boreal shrub	*Salix*	0.034 [2]	1.209 (0.039)
V	boreal shrub	Ericaceae	0.034 [4]	0.200 (0.029)
VI	arid-tolerant shrub and herb	*Ephedra*	0.015 [8]	0.960 (0.140)
VI	arid-tolerant shrub and herb	*Artemisia*	0.014 [6]	9.072 (0.176)
VI	arid-tolerant shrub and herb	Chenopodiaceae	0.019 [6]	5.440 (0.460)
VII	grassland and tundra forb	Poaceae	0.035 [4]	1.000 (0.000)
VII	grassland and tundra forb	Cyperaceae	0.035 [5]	0.757 (0.044)

VII	grassland and tundra forb	Asteraceae	0.051 [7]	0.465 (0.066)
VII	grassland and tundra forb	*Thalictrum*	0.007 [8]	3.855 (0.258)
VII	grassland and tundra forb	Ranunculaceae	0.014 [9]	2.900 (0.363)
VII	grassland and tundra forb	Caryophyllaceae	0.028 [9]	0.600 (0.050)
VII	grassland and tundra forb	Brassicaceae	0.002 [3]	4.185 (0.188)

[1] Eisenhut (1961); [2] Gregory (1973); [3] Li et al. (2017); [4] Broström et al. (2004); [5] Sugita et al. (1999); [6] Abraham and Kozáková (2012); [7] Broström et al. (2002); [8] Xu et al. (2014); [9] Bunting et al. (2013).

2.2 The REVEALS model setting

The REVEALS model assumes the PPEs of pollen taxa are constant variables over the target period, and requires parameter inputs including sediment basin radius (m), fall speed of pollen grain (FS, m/s), and PPE with standard error (SE; Sugita, 2007). The areas of the 110 lakes were obtained from descriptions in original publications and validated by measurements on Google Earth. Their basin radii were back-calculated from their areas assuming a circular shape. There are 83 large lakes (radius >390 m; following Sugita, 2007) in our dataset with a fairly even distribution across the study area (Fig. 1; Appendix 1), which helps ensure the reliability of the regional vegetation estimations (Sugita, 2007; Mazier et al., 2012). Only 18 bogs have published descriptions about their size and it is infeasible to measure them on Google Earth because of unclear boundaries. A test-run showed that using different bog radii (i.e. 5 m, 10 m, 20 m, 50 m, 100 m, 200 m and 500 m) did not significantly affect the REVEALS estimates (Appendix 3), hence a standard (moderate size) radius of 100 m was set for all bogs.

We collected available PPEs for the 27 selected pollen taxa from 20 studies in Eurasia (Appendix 4). We calculated the mean PPE from all available PPE values, but excluded records with PPE ≤ SE (Mazier et al., 2012). We included these PPEs for various species in the mean PPE calculation for their family or genus. For simplification, we did not evaluate the values or select PPE values following consistent criteria as was done in Europe (Mazier et al., 2012). Instead, we used the original values from the studies included in Mazier et al. (2012) and added new PPE values from Europe published since the synthesis of Mazier et al. (2012). SE of the

mean PPE was estimated using the delta method (Stuart and Ord, 1994). Fall speeds for each of the 27 pollen taxa were retrieved from previous studies (Table 2).

The REVEALS model generally performs best with pollen records from large lakes, although multiple pollen records from small lakes and bogs (at least two sites) can also produce reliable results where large lakes are absent (Sugita, 2007; Trondman et al., 2016). Here, due to the sparse distribution of available sites, we divided the 203 sites into 42 site-groups, based on criteria of geographic location, vegetation type (vegetation zone map modified from Tseplyayev, 1961; Dulamsuren et al., 2005; Hou, 2001), climate (based on modern precipitation and temperature contours), and permafrost (Brown, 1997) following the strategy of Li (2016), and the pollen data within one site-group should be of similar components and temporal patterns. To ensure the reliability of REVEALS estimates of plant cover, each group includes at least one large lake or two small sites (small lakes or bogs; Fig. 1; Appendix 5).

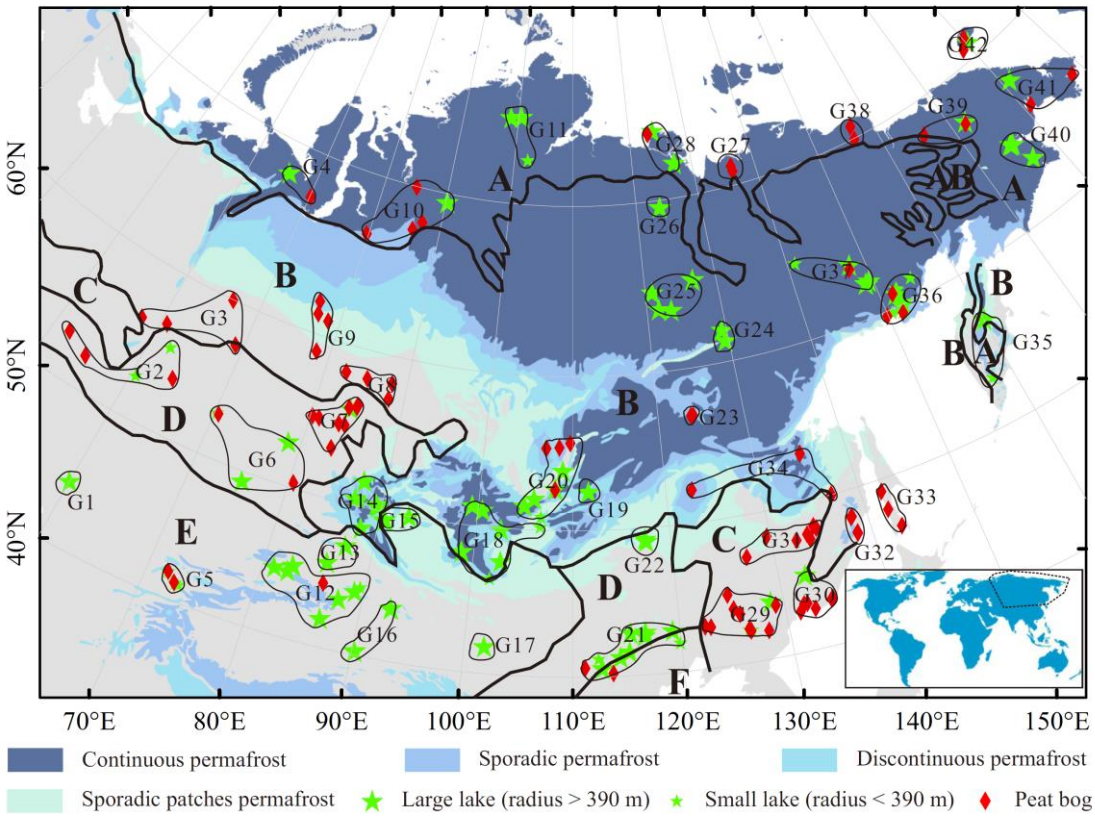

Fig. 1. Distribution of the 42 site-groups together with the modern vegetation zones and permafrost extent in northern Asia. The vegetation-zone map modified from Tseplyayev (1961), Dulamsuren et al. (2005), and Hou (2001) includes: A: tundra, B: taiga forest, C: temperate mixed

conifer-deciduous broadleaved forest, D: temperate steppe, E: semi-desert and desert; F: warm-temperate deciduous forest.

The REVEALS model was run with a mean wind speed set to 3 m/s and neutral atmospheric conditions following Trondman et al. (2015), and the maximum distance of regional vegetation *Zmax* was set to 100 km. The lake and bog sites were reconstructed using the models of pollen dispersal and deposition for lakes (Sugita, 1993) and bogs (Prentice, 1985), respectively in REVEALS version 5.0 (Sugita, unpublished). The mean estimate of plant abundances from lakes and bogs was calculated for each of the 42 site-groups, which includes both sediment types (using the computer program bog.lake.data.fusion, Sugita, unpublished). Finally, the 27 taxa were assigned to seven plant functional types (PFT; Table 1) following the PFT definitions for China and Siberia (Tarasov et al. 1998, 2000; Bigelow et al. 2003; Ni et al., 2010; Tian et al., 2017), with the restriction that each pollen taxon is attributed to only one PFT according to the strategy of Li (2016) (Table 2).

2.2 Numerical analyses of reconstruction

The abundance variations of the seven PFTs during the Holocene (time slices between 12 and 1 ka) from 34 site-groups were used in a clustering analysis. Eight site-groups had to be excluded from the analysis due to poor coverage of time slices (G1, G5, G17, G19, G27, G42). For site-groups with <3 missing time slices during the Holocene (G3, G16, G26, G32, G33, G35, G38, G39, G41), linear interpolation was employed to estimate the PFT abundances for the missing time slices. Time-series clustering for the three-way dataset was performed to generate a distance matrix among the site-groups using the *tsclust* function in the *dtwclust* package (Sarda-Espinosa, 2018) in R 3.4.1 (R Core Team, 2017). The distance matrix was employed in hierarchical clustering (using the *hclust* function in R) to cluster the site-groups. Constrained hierarchical clustering (using *chclust* function in *rioja* package version 0.9-15.1; Juggins, 2018) was used to determine the timing of primary vegetation changes (i.e. the first split) in each site-group. A change was considered to

be significant when the split passed the broken-stick test. The amount of PFT compositional change (turnover) through time during the period between 12 and 1 ka for the 34 site-groups (their time slices or interpolated ones can cover entire period) was estimated by detrended canonical correspondence analysis (DCCA) for each site-group (ter Braak, 1986) using CANOCO 4.5 (ter Braak and Šmilauer, 2002).

3. Results

Large-scale pattern

On a glacial-interglacial scale, marked temporal changes in the occurrence and abundance of PFTs are revealed, in particular the high cover of tree PFTs during the Holocene as opposed to the widespread open landscape during the glacial period. In contrast, vegetation changes in northern Asia within the Holocene are rather minor with only slight changes in PFT abundances. Cluster analyses of grouped vegetation records from the Holocene find five clusters (Appendix 6). Their spatial distribution is largely consistent with the distribution of modern vegetation types as characterized by certain PFTs. (1) Records from the forest-steppe ecotone (e.g. G12, G21; Fig. 2A) in north-central China and the Tianshan Mts. (the mentioned geographic locations are indicated in Appendix 7) have high tree PFTs during the middle Holocene. (2) Areas in southern and south-western Siberia and north-eastern China were covered by cool-temperate mixed forest or light taiga with a high diversity of trees throughout the Holocene (e.g. G2, G7, G14, G29; Fig. 2B). (3) The West Siberian Plain and south-eastern Siberia that are presently covered by open dark taiga forests (e.g. G8, G9, G33; Fig. 2C) had an even higher abundance of evergreen conifer trees during the middle Holocene than at present. (4) *Larix* formed light taiga forests in central Yakutia throughout the Holocene (e.g. G25, G26; Fig. 2D). (5) Northern Siberia, which is currently covered by tundra formed by boreal shrubs and herbs, had a higher share of tree PFTs during the middle Holocene (e.g. G28, G39; Fig. 2E).

The turnover in PFT composition is <0.7 SD units in almost all site-groups, except G8 (0.88 SD), G9 (0.73 SD), and G24 (0.76 SD), indicating only slight vegetation change

during the Holocene (Fig. 3). The three site-groups with higher turnover show a distinct transition from light taiga to dark taiga in the middle Holocene (at ca. 8 ka). This result is consistent with the finding that PFT abundance from 16 site-groups shows no significant temporal clusters. The primary vegetation changes (i.e. all significant splits or, if no significant split occurs in a record, the first insignificant split) occur during different intervals in each site-group. Overall, the early Holocene (including 11.5, 10.5, and 9.5 ka time-slices) has the highest frequency of primary vegetation changes. Records from the south-eastern coastal part of the study area are characterized by relatively many early-Holocene splits (e.g. G29, G30, G32, G33, G34, G36, G37). There are 16 site-groups whose primary vegetation changes during the middle Holocene (including 8.5, 7.5, 6.5, and 5.5 ka time-slices), and most of them are from inland areas such as the West Siberian Plain, central Yakutia, and northern Mongolia. Only seven site-groups have late-Holocene primary vegetation changes (Fig. 3).

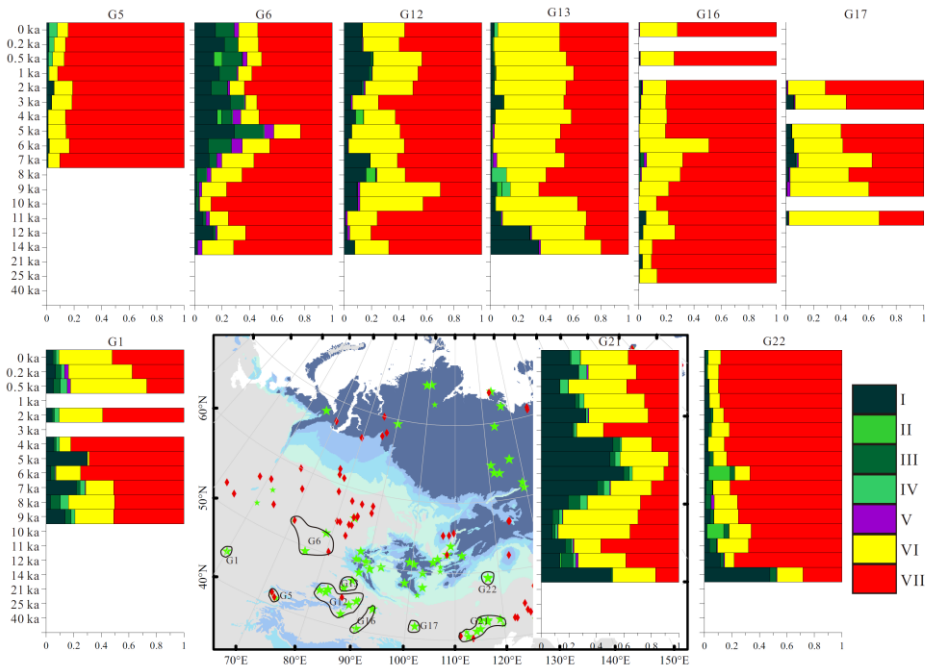

Fig. 2A. Temporal changes of plant functional type (PFT) cover, as proportions, for the site-groups from the warm temperate forest margin zone. PFT I: evergreen conifer tree; PFT II: deciduous conifer tree; PFT III: boreal deciduous tree; PFT IV: temperate deciduous tree; PFT V: boreal shrub; PFT VI: arid-tolerant shrub and herb; and PFT VII: steppe and tundra forb.

Warm temperate forest margin zone in vicinity of Tianshan Mts. and north-central China (G6, G12, G13, G16, G21, G22)

Six site-groups from the warm temperate forest-steppe transition zone (G6, G21, G22) and from the lowlands adjacent to mountainous forest in arid central Asia (G12, G13, G16) are clustered together (Fig. 3). Our results indicate that these areas, which are now dominated by arid-tolerant shrub and steppe species, had more arboreal species, mainly evergreen conifer tree taxa, in the middle Holocene (Fig. 2A). For example, north-central China (G21) has a marked mid-Holocene maximum in forest cover (7–4 ka; mean 51%). However, certain peculiarities are noted: open landscape is reconstructed between 14 and 7 ka in northern Kazakhstan (G6), followed by an abundance of evergreen conifer trees and an increase in boreal deciduous trees that maintain high values (mean 30%) after 7 ka. In the eastern branch of the Tianshan Mts. (G12), evergreen conifer trees are highly abundant from 10 to 7 ka and after 2 ka, while low abundance occurs from 14 to 11 ka and from 6 to 3 ka. In the Gobi desert near the Tianshan Mts. (G16) there was an even higher abundance of arid-tolerant species with no notable temporal trend in abundance of arboreal species. We assume that the high arboreal cover at site-groups G13 and G22 at 14 and 12 ka originates from riverine transport and therefore exclude them from further analyses.

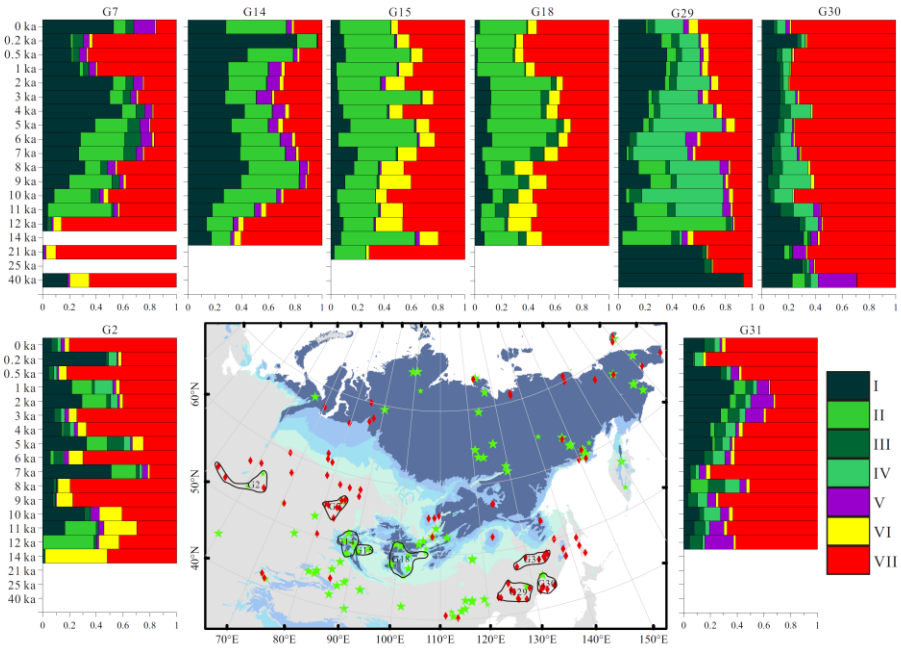

Fig. 2B. Temporal changes of plant functional type (PFT) cover, as proportions, for the site-groups from cool-temperate mixed forest and taiga forest. PFT I: evergreen conifer tree; PFT II: deciduous conifer tree; PFT III: boreal deciduous tree; PFT IV: temperate deciduous tree; PFT V: boreal shrub; PFT VI: arid-tolerant shrub and herb; and PFT VII: steppe and tundra forb.

Cool-temperate mixed forest and taiga forest in southern and south-western Siberia and north-eastern China (G2, G7, G14, G15, G18, G29, G30, G31)

Eight site-groups located in (or near) the temperate mixed conifer-deciduous broadleaved forest zone (G2, G29, G30, G31) and taiga-steppe transition zone (G7, G14, G15, G18) show similar PFT compositions and temporal evolutions. At these sites, evergreen conifer tree is the dominant PFT intermixed with other arboreal PFTs, such as deciduous conifers (*Larix*) in the Altai Mts. and northern Mongolia, and/or temperate deciduous trees in north-eastern China (Fig. 2B).

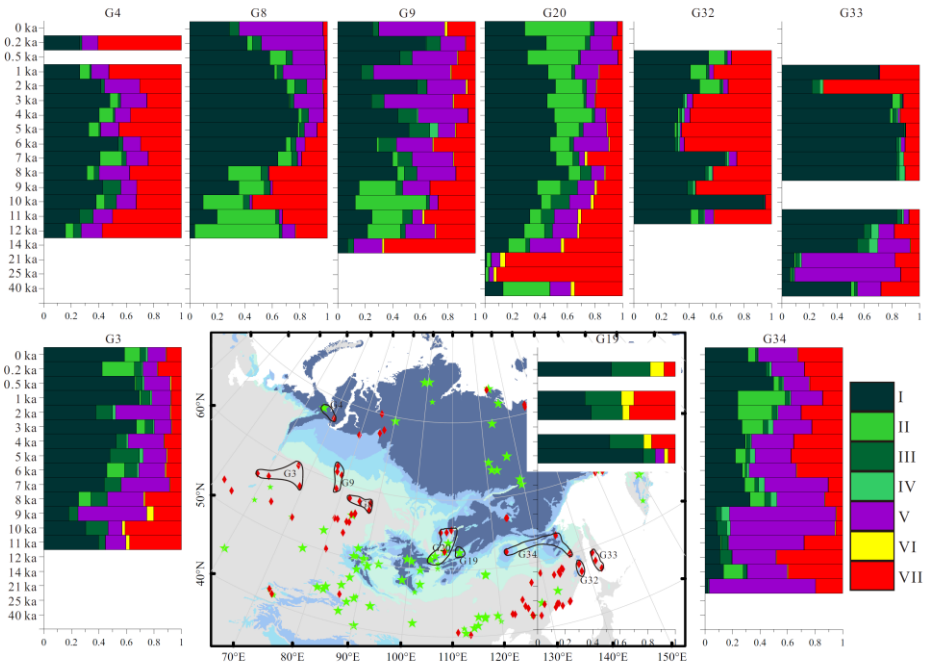

Fig. 2C. Temporal changes of plant functional type (PFT) cover, as proportions, for the site-groups from dark taiga forest. PFT I: evergreen conifer tree; PFT II: deciduous conifer tree; PFT III: boreal deciduous tree; PFT IV: temperate deciduous tree; PFT V: boreal shrub; PFT VI: arid-tolerant shrub and herb; and PFT VII: steppe and tundra forb.

Evergreen conifer tree is the dominant PFT at 40, 25, and 21 ka in the southern part of

north-eastern China (G29), *Larix* then becomes the dominant taxa at 14 and 12 ka, and temperate deciduous trees increase thereafter and maintain high cover between 11 and 3 ka. After 2 ka, evergreen conifer trees increase to 32% on average while temperate deciduous trees decrease to 18% on average. While arboreal abundance is lower in the northern part of north-eastern China (G30, G31) than in the southern part (G29), it shows a similar temporal pattern (Fig. 2B).

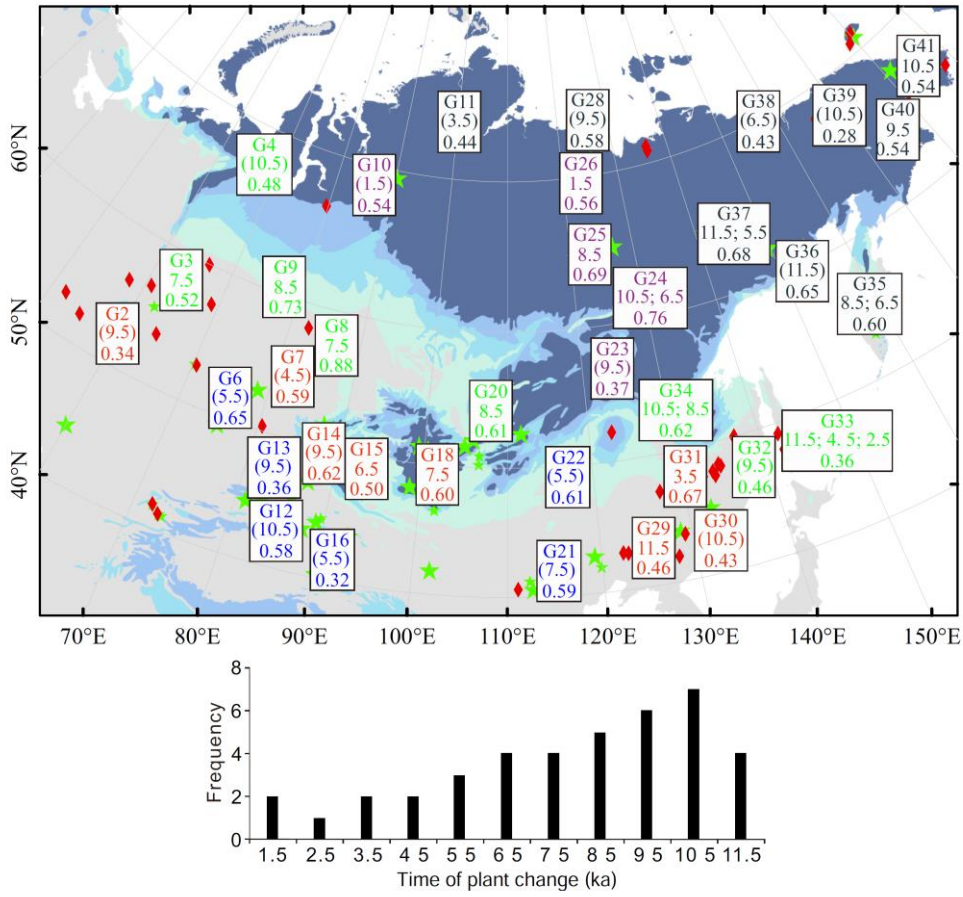

Fig. 3. Clustering results of the 34 site-groups represented by the colour of the boxes, with the age of primary vegetation changes (middle row of each box; data in brackets means the hierarchical clustering failed the broken-stick test) and the compositional change (turnover; lower row) during the Holocene. A summary of the frequency of when the primary vegetation changes (revealed by constrained hierarchical clustering, including significant and insignificant once) occurred is provided below the map.

Open landscape is revealed for the southern Ural region (G2) with high abundances of herbaceous species at 14 ka. The cover of *Larix* and evergreen conifer trees increases

after 12 ka and maintains high values thereafter with no notable temporal trend (Fig. 2B).

In the taiga-steppe transition zone, *Larix* is the dominant arboreal taxon, particularly in the northern Altai Mts. and northern Mongolia (G15, G18). Open landscapes are inferred at 40, 21, and 12 ka on the southern West Siberian Plain (G7); cover of *Larix* increases at 11 ka, and evergreen conifer trees increase from 9 ka and become the dominant forest taxon after 4 ka. The temporal pattern of evergreen conifer trees in the Altai Mts. (G14) is similar to the southern West Siberian Plain, although *Larix* maintains high abundances into the late Holocene. Relative to the Altai Mts., the abundance of evergreen conifer trees for all time windows are lower in the area north of the Altai Mts. and in northern Mongolia (G15, G18), but their temporal change patterns are consistent with those of the Altai Mts. (G14; Fig. 2B).

Dark taiga forest in western and south-eastern Siberia (G3, G4, G8, G9, G20, G32, G33, G34)

Site-groups with dark taiga forest from western Siberia (G3, G4, G8, G9), the Baikal region (G20), and south-eastern Siberia (G32, G33, G34) form one cluster sharing similar PFT compositions dominated by evergreen conifer trees, with *Larix* and boreal broadleaved shrubs as the common woody taxa during the Holocene (Fig. 2C).

On the West Siberian Plain (G8, G9), high cover of *Larix* is reconstructed during the early Holocene as well as high woody cover since the middle Holocene formed by evergreen conifer trees and boreal shrubs. In the Ural region (G3, G4), evergreen conifer trees dominate the arboreal species throughout the Holocene. The absence of *Larix* in the early Holocene in this Ural region is a notable difference to the West Siberian Plain (Fig. 2C).

In the Baikal region (G20), relatively closed landscape is revealed at 40 ka; openness then increases to >95% at 25 and 21 ka. Since 14 ka, woody cover increases as shown by a notable rise in evergreen conifer trees from 14 to 8 ka and by increases of *Larix* after 7 ka (Fig. 2C).

In south-eastern Siberia (G32, G34), arboreal abundance is high in the early and late Holocene, but low in the middle Holocene. South of Sakhalin Island (G33), closed landscape is revealed between 40 and 1 ka with >80% woody cover. Evergreen conifer tree PFT has lower cover than boreal shrub PFT at 25 and 21 ka, but increases in abundance around 14 ka rising to 83% on average between 11 and 3 ka, and reduces thereafter (Fig. 2C).

Light taiga forest in north-western Siberia and central Yakutia (G10, G23, G24, G25, G26)

Plant composition of this cluster is dominated by *Larix* with high arboreal cover during the Holocene. Evergreen conifer trees are present at ca. 15% cover between 11 and 2 ka, with high arboreal values (mean 73%) during the Holocene in north-western Siberia (G10). In central Yakutia (G23, G24, G25), evergreen conifer trees increase markedly from ca. 8 ka, 6 ka, and 7 ka, respectively and maintain high cover thereafter, with ca. 60% arboreal cover throughout the Holocene. Evergreen conifer trees are almost absent in the taiga-tundra ecotone (G26; Fig. 2D).

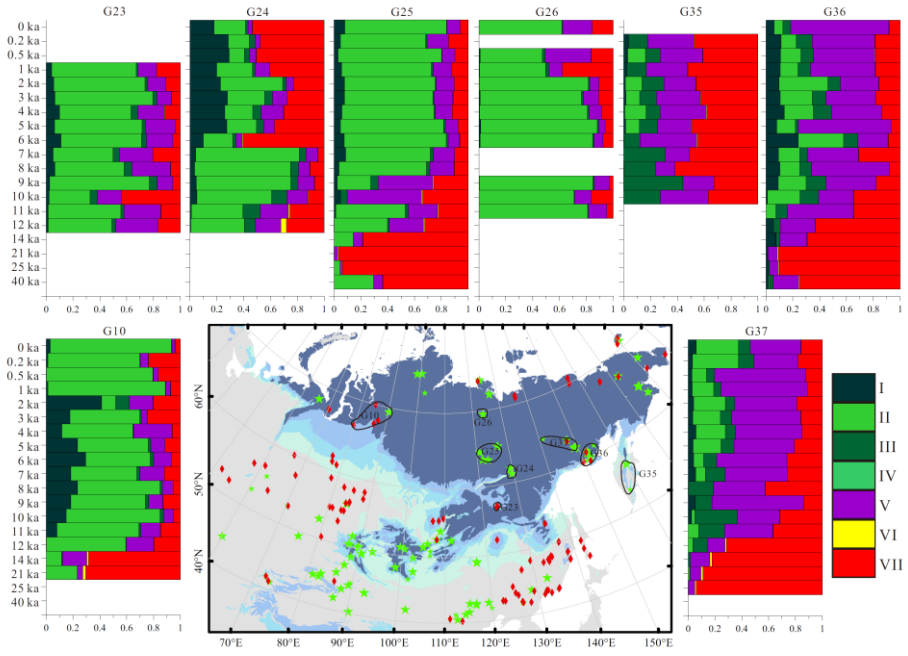

Fig. 2D. Temporal changes of plant functional type (PFT) cover, as proportions, for the site-groups from light taiga forest and taiga-tundra ecotone (G35, G36, G37). PFT I: evergreen conifer tree; PFT II: deciduous conifer tree; PFT III: boreal deciduous tree; PFT IV: temperate deciduous tree;

PFT V: boreal shrub; PFT VI: arid-tolerant shrub and herb; and PFT VII: steppe and tundra forb.

Tundra on the Taymyr Peninsula and taiga-tundra ecotone in north-eastern Siberia (G11, G28, G35, G36, G37, G38, G39, G40, G41)

Plant compositions of this cluster are characterized by high abundances of boreal shrubs and tundra forbs. *Larix* is the only tree species on the Taymyr Peninsula (G11) and its abundance increases from 18% at 14 ka to 60% at 10 ka, and then decreases to 18% at 5 ka. The landscape of the north Siberian coast (G28) is dominated by shrub tundra from 14 ka to 10 ka, then *Larix* increases sharply and maintains high values between 9 and 6 ka. After 5 ka, *Larix* reduces, and shrub tundra becomes the dominant landscape again (Fig. 2E).

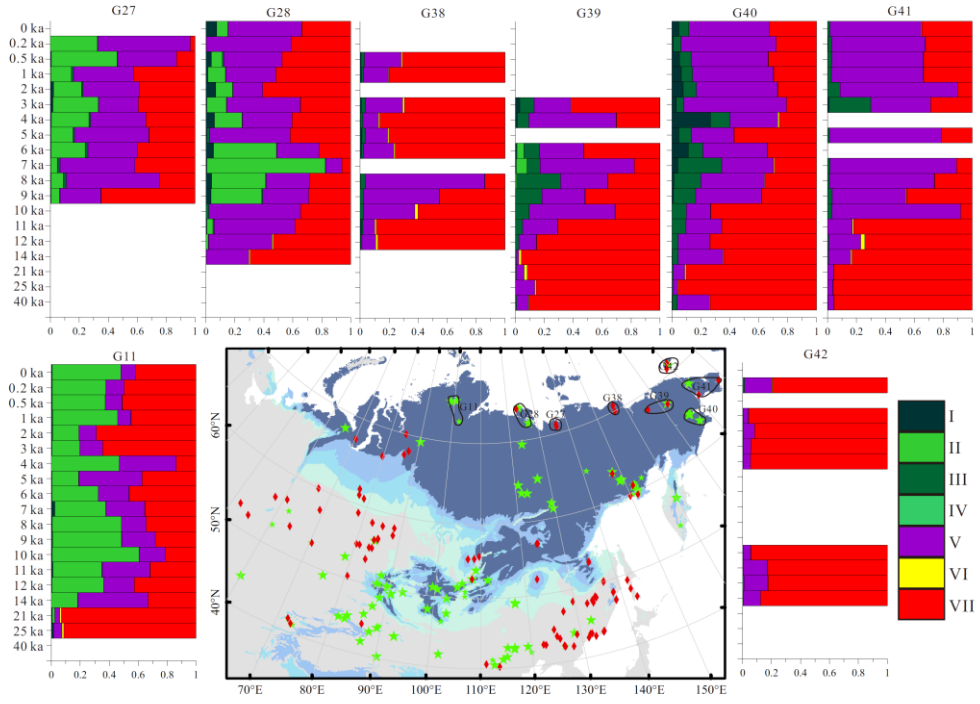

Fig. 2E. Temporal changes of plant functional type (PFT) cover, as proportions, for the site-groups from tundra and taiga-tundra ecotone. PFT I: evergreen conifer tree; PFT II: deciduous conifer tree; PFT III: boreal deciduous tree; PFT IV: temperate deciduous tree; PFT V: boreal shrub; PFT VI: arid-tolerant shrub and herb; and PFT VII: steppe and tundra forb.

In north-eastern Siberia, arboreal cover shows a decreasing trend from southerly site-groups (G35, G36, G37; Fig. 2D) to northerly ones (G40, G38, G39, G41) following the increasing latitude. In the Olsky District, temporal patterns of vegetation

changes in G37 are consistent with G36, with stable vegetation during the Holocene and increases in evergreen conifer tree abundance from ca. 9 ka. Arboreal composition on the southern Kamchatka Peninsula (G35) is dominated by boreal deciduous trees during the first stage of the Holocene, followed by rising abundances of *Larix* and evergreen conifer trees from 5 ka.

In north-eastern Siberia (G40, G38, G39, G41), the landscape is dominated by forb tundra with sparse shrubs between 40 and 21 ka; the cover of shrubs increases at 14 ka and arboreal cover (dominated by boreal deciduous trees) increases in the early Holocene (11 or 10 ka). Shrubs maintain a high abundance throughout the Holocene, while trees peak between 10 and 2 ka generally (Fig. 2E).

4. Discussion

4.1 Land-cover changes and potential biases

The overall patterns of pollen-based REVEALS estimates of land cover are generally consistent with previous vegetation reconstructions. Although only a few site-groups cover the period from 40 to 21 ka, a consistent vegetation signal indicates that relatively closed landscapes occurred in south-eastern Siberia, north-eastern China, and the Baikal region (Fig. 2), while most of Siberia was rather open, particularly around 21 ka (Fig. 2). These findings are consistent with previous pollen-based (Tarasov et al., 1998, 2000; Bigelow et al., 2003; Binney et al. 2017; Tian et al., 2018) and model-estimated biome reconstructions (Tian et al., 2018). During the late Pleistocene (40, 25, 21, 14 ka), steppe PFT abundance was high in central Yakutia and north-eastern Siberia (e.g. G25, G36, G37, G39, G40, G41), which may reflect the expansion of tundra-steppe, consistent with results from ancient sediment DNA which reveal abundant forb species during the period between 46 and 12.5 ka on the Taymyr Peninsula (Jørgensen et al., 2012). The tundra-steppe was replaced by light taiga in southern Siberia and by tundra in northern Siberia at the beginning of Holocene or the last deglaciation, which is consistent with ancient DNA results (forbs-dominated steppe-tundra; Willerslev et al., 2014).

During the Holocene, reconstructed land cover for each site-group is generally consistent with their modern vegetation. The slight vegetation changes are represented by changes in PFT abundances rather than by changes in PFT presence/absence. Minor changes are also indicated in the cluster analysis, which shows that plant compositions and their temporal patterns are consistent among the site-groups within the same modern vegetation zone (Fig. 3). PFT datasets from 16 site-groups fail the broken-stick test for clustering analysis, and most of the remaining site-groups have only one significant vegetation change, further supporting the case that only slight changes occurred during the Holocene in northern Asia. In addition, the low total amount of PFT change (turnover) over the Holocene for most site-groups supports the view of slight temporal changes in land cover.

Vegetation turnover on the Tibetan Plateau inferred from pollen percentages is documented to overestimate the strength of vegetation changes (Wang and Herzschuh, 2011). This matches with our results. In central Yakutia, the pollen percentage data indicate a strong vegetation change during the middle Holocene, represented by a sharp increase of *Pinus* pollen, but the strength of the vegetation change is overestimated because of the high PPE of *Pinus*. The PPE-corrected arboreal abundances in central Yakutia after ca. 7 ka with ca. 70% *Larix* and ca. 10% *Pinus* are consistent with modern light taiga (Katamura et al., 2009). Furthermore, the absence of *Pinus* macrofossils in central Yakutia throughout the Holocene (Binney et al., 2009) also suggests a restricted distribution of *Pinus*, possibly to sandy places such as river banks (Isaev et al., 2010).

Pollen-based turnover estimates from southern Norway range between 0.84 to 1.3 SD (mean 1.02 SD) for ten Holocene pollen spectra (Birks, 2007), and from northern Europe between 0.01 (recent) to 0.99 (start of the Holocene) SD for three sites (N Sweden, NW and SE Finland) (Marquer et al., 2014). Moreover, the REVEALS-based turnover estimates (0.3–1) for northern Europe are significantly higher than the pollen-based one (0.2–0.8) from 11 ka to 5.5 ka BP. The same is true for all other regions studied by Marquer et al. (2014) in north-western Europe, and the turnover

estimates (pollen- and REVEALS-based) are generally higher at lower latitudes from southern Sweden down to Switzerland and eastwards to Britain and Ireland. These European values are higher than our REVEALS-based turnover estimates (from 0.37 to 0.88 SD, mean 0.66 SD; G3, G8, G9, G23, G24, G25, G36, G37) from a similar latitudinal range (Fig. 3). The fewer parameters used in the turnover calculations for northern Asia (PFTs) compared to Europe (pollen taxa) is a potential reason for the lower turnover obtained in this study. In addition, the PPE-based transformation from pollen percentages to plant abundances may reduce the strength of vegetation changes (Wang and Herzschuh, 2011). Aside from the methodological aspects, the lower turnover in northern Asia may, at least partly, originate from differences in the environmental history between northern Europe compared with northern Asia, that is glaciation followed by postglacial re-vegetation vs. non-glaciated areas with trees in refugia, respectively, and a maritime climate with temperature-limited vegetation distribution vs. a continental climate with temperature- and moisture-limited vegetation.

We consider the REVEALS-based regional vegetation-cover estimations in this study as generally reliable with reasonable standard errors (Appendix 8) thanks to the thorough selection of records with high quality pollen data and reliable chronologies. In addition, the landscape reconstructions are generally consistent with previous syntheses of past vegetation change (e.g. Tian et al., 2018) and known global climate trends (Marcott et al., 2013), plus the clustering results of PFT abundance are consistent with modern spatial vegetation patterns. That said, this study faced two major methodological challenges, discussed below, that may reduce the reliability of the obtained quantitative land-cover reconstructions; 1) the low number of PPEs and their origin and 2) restrictions with respect to the number, distribution, and type of available sites.

(1) Twenty PPE sets were used which mostly originate from Europe and temperate northern China. The available PPEs were estimated from various environmental and ecological settings, which might cause regional differences

in each PPE. And, PPEs of different species within one family or genus were included in our mean PPE calculation for the family or genus, ignoring the inter-species differences. Also, some taxa behave few available PPEs with significant differences (such as *Abies*, *Larix*, *Juglans*, Brassicaceae), and their mean PPE could fail to represent their real pollen productivities. These aspects can cause uncertainty in the mean PPE to some extent. However, we believe that the compiled PPE sets can be used to extract major broad-scale and long-term vegetation patterns because the regional differences in the PPE for most taxon are small compared to the large between-taxa differences. The mean PPEs used in this REVEALS modelling (Table 2) are broadly consistent with those obtained from Europe (Mazier et al., 2012). In addition, although there are no PPEs for the core from the Siberia taiga forest, available studies on modern pollen composition support the weightings in the applied PPEs for major taxa in terms of pollen under- or over-representation of vegetation abundance. For example, modern pollen investigations in north-eastern Siberia revealed that pollen records from northern *Larix* forest often have less than 13% *Larix* pollen, confirming the low pollen productivity of *Larix* relative to over-represented pollen taxa such as *Betula* and *Alnus* (Pisaric et al., 2001, Klemm et al., 2016). Similarly, a study on modern pollen in southern Siberia (transitional area of steppe and taiga) finds that *Artemisia*, *Betula*, and *Pinus* are high pollen producers compared to *Larix* (Pelánková et al., 2008). Also, despite *Larix* being the most common tree in taiga forest in north-central Mongolia, the pollen abundance of *Larix* is generally lower than 3% (Ma et al., 2008), implying its low pollen productivity.

(2) In this study, we attempt to reconstruct past landscape changes at a regional scale. Pollen signals from large lakes are assumed to reflect regional vegetation patterns (e.g. Sugita et al., 2010; Trondman et al., 2015). If large lakes are absent in a region, multiple small-sized sites can be used, although error estimates are usually large (Sugita, 2007; Mazier et al., 2012; Trondman

et al., 2016). In our study, 70% of the time slices for the 42 site-groups include pollen data from large lakes (i.e. radii >390m), which supports the reliability of REVEALS reconstructions (Appendix 5). However, sites are unevenly distributed and occasionally sites from different areas were combined into one group (G2, G6, G34), which might produce a different vegetation-change signal because of the broad distribution of these sites (Fig. 1). In addition, the linear interpolation of pollen abundances for time windows with few pollen data might be another source of uncertainty, particularly for the late Pleistocene and its broad time windows (Table 1). Finally, pollen signals from certain sites and during certain periods may be of water-runoff origin rather than aerial origin violating the assumption of the REVEALS-model that pollen is transported by wind.

4.2 Driving factors of vegetation changes

On a glacial-interglacial scale, pollen-based reconstructed land-cover changes in northern Asia are generally consistent with the global climate signal (e.g. sea-surface temperature: Pailler and Bard, 2002; ice-core: Andersen et al., 2004; solar insolation: Laskar et al., 2004; cave deposits: Cheng et al., 2016; Appendix 9). For example, the relatively high arboreal cover at 40 ka (e.g. G20) corresponds with the warm MIS3 record from the Baikal region (Swann et al., 2005). The open landscape at 25 ka and 21 ka (e.g. G25, G36) reflects the cold and dry last glacial maximum (e.g. Swann et al., 2010). Furthermore, the relatively high arboreal cover during the Holocene is consistent with the warm and wet climate (occurring in most site-groups). The primary vegetation change in north-eastern China (G29, G30) occurs in the early Holocene (11.5 and 10.5 ka), caused by the rapid increase in abundance of temperate deciduous trees, which may reflect the warmer climate and enhanced summer monsoon known from that region at the beginning of the Holocene (Hong et al., 2009, Liu et al., 2014).

A sensitivity analysis of model-based biome estimation reveals that precipitation plays an important or even dominant role in controlling vegetation changes in arid central

Asia (e.g. Tian et al., 2018). The climate of central Asia during the early Holocene is inferred to be quite dry and moisture increase occurs at ca. 8 ka revealed by a series of multi-proxy syntheses (Chen et al., 2008, 2016; Xie et al., 2018) and model-based estimations (Jin et al., 2012). In the taiga-steppe transition zone (south-eastern Siberia and north-central Asia; e.g. G6, G12, G14, G18), relatively open landscape is reconstructed for the early Holocene and abundances of forest taxa increase after ca. 8 ka, which are consistent with the moisture evolution, and imply the importance of moisture in controlling vegetation changes. Our results support the prediction of an expansion of steppe in the present forest–steppe ecotone of southern Siberia in response to a warmer and drier climate in the future (Tchebakova et al., 2009). During the late Holocene, the decreases in forest cover in the forest–steppe ecotone of north-central China and central Asia are ascribed to the drying or cooling climate respectively by sensitivity analysis (Tian et al., 2018). However, the enhanced human impacts might be another important factor (e.g. Ren, 2017), while the model fail to separate its contribution on vegetation.

High abundances of *Larix* or boreal deciduous woody taxa (mostly shrubs) pollen occur in northern Siberia (e.g. G28, G38, G39, G40) during the middle Holocene, which is now covered by tundra. This is consistent with non-vegetation climate records of a mid-Holocene temperature maximum (e.g. Biskaborn et al, 2012; Nazarova et al., 2013). This result indicates that the boreal treeline in northern Siberia reacts sensitively to warming on millennial time-scales, which contrasts with the observed lack of response on a decadal time-scale (Wieczoreck et al., 2017). This may point to a highly non-linear vegetation–climate relationship in northern Siberia.

Our results indicate that climate change is the major factor driving land-cover change in northern Asia on a long temporal scale. However, climate change cannot fully explain the changes in arboreal taxa abundance for the West Siberian Plain (G8, G9) and sandy places in central Yakutia (G23, G24, G25). In addition to climate, changes in permafrost condition (Vandenberghe et al., 2014) and fire regime may have played a central role in vegetation change. *Larix* is the dominant arboreal taxon during the

early Holocene (ca. between 12 and 8 ka), which is replaced by evergreen conifer trees, mostly pine and spruce at 8 or 7 ka. *Larix* can survive on permafrost with an active-layer depth of <40 cm (Osawa et al., 2010) and a high fire frequency, while pine trees can only grow on soil with >1.5m active-layer (Tzedakis and Bennett, 1995) and spruce is a fire-avoider. Probably the compositional change of boreal trees was not in equilibrium with climate but rather driven by changes in the permafrost and fire characteristics that were themselves affected by forest composition, resulting in complex feedbacks. This explanation would be in agreement with the finding of Herzschuh et al. (2016) that the boreal forest composition of nearby refugia during a glacial influences the initial interglacial forest composition that is then only slowly replaced by a forest composition that is in equilibrium with climate.

Population changes of herbivores could also be an important factor for vegetation change at a regional scale during certain intervals (Zimov et al., 1995; Guthrie, 2006). As with our pollen-based land-cover reconstruction, a circumpolar ancient DNA metabarcoding study confirms the replacement of steppe-like tundra by moist tundra with abundant woody plants at the Pleistocene–Holocene transition (Willerslev et al., 2014). According to Zimov et al. (1995, 2012), such a change cannot be explained by climate change alone, and thus a reduced density of herbivores is considered to be a major driving factor of steppe composition reduction, since a reduced number of herbivores is insufficient to maintain the open steppe landscapes and so causes a decrease in steppe area (Zimov et al., 1995; Guthrie, 2006). Our land-cover reconstruction fails to address the contribution of herbivores to vegetation changes, but the extinction of herbivorous megafauna would add to the complexity of the interactions among vegetation, climate and permafrost.

5. Conclusions

Regional vegetation based on pollen data has been estimated using the REVEALS model for northern Asia during the last 40 ka. Relatively closed land cover was replaced by open landscapes in northern Asia during the transition from MIS 3 to the

last glacial maximum. Abundances of woody components increase again from the last deglaciation or early Holocene. Pollen-based REVEALS estimates of plant abundances should be a more reliable reflection of the vegetation as pollen may overestimate the turnover, and indicates that the vegetation was quite stable during the Holocene as only slight changes in the abundances of PFTs were recorded rather than mass expansion of new PFTs. From comparisons of our results with other data we infer that climate change is likely the primary driving factor for vegetation changes on a glacial-interglacial scale. However, the extension of evergreen conifer trees since ca. 8–7 ka throughout Siberia could reflect vegetation-climate disequilibrium at a long-term scale caused by the interaction of climate, vegetation, fire, and permafrost, which could be an palaeo-analogue not only for the recent complex vegetation response to climate changes but also for the vegetation prediction in future.

Data availability. The used fossil pollen dataset with the re-established age-depth model for each pollen record have been made publicly available in Pangaea (https://doi.pangaea.de/10.1594/PANGAEA.898616).

Acknowledgements. The authors would like to express their gratitude to all the palynologists who, either directly or indirectly, contributed their pollen records and PPE results to our study. This research was supported by the German Research Foundation (DFG) and PalMod project (BMBF). FL and MJG thank the Faculty of Health and Life Science of Linnaeus University (Kalmar, Sweden), the China-Swedish STINT Exchange Grant 2016-2018 and the Swedish Strategic Research Area on ModElling the Regional and Global Earth system (MERGE) for financial support. This study is a contribution to the Past Global Changes (PAGES) LandCover6k working group project.

References

Abaimov, A.P., Prokushkin, S.G., Matssura, Y., Osawa, A., Takenaka, A., and Kajimoto, T.: Wildfire and cutting effect on larch ecosystem permafrost dynamics in central Siberia, in Shibuya, M., Takanashi, K., Inoue, G. (eds.), Proceedings of

599 the Seventh Symposium on the Joint Siberian Permafrost Studies between Japan
600 and Russia in 1998, Tsukuba, Japan, 48–58pp., 1999.
601 Abraham, V. and Kozáková, R.: Relative pollen productivity estimates in the modern
602 agricultural landscape of Central Bohemia (Czech Republic), Review of
603 Palaeobotany and Palynology, 179, 1–12, 2012.
604 Andersen, K.K., Azuma, N., Barnola, J.-M., Bigler, M., Biscaye, P., Caillon, N.,
605 Chappellaz, J., Clausen, H.B., Dahl-Jensen, D., Fischer, H., Flückiger, J.,
606 Fritzsche, D., Fujii, Y., Goto-Azuma, K., Grenvold, K., Gundestrup, N.S.,
607 Hansson, M., Huber, C., Hvidberg, C.S., Johnsen, S.J., Jonsell, U., Jouzel, J.,
608 Kipfstuhl, S., Landais, A., Leuenberger, M., Lorrain, R., Masson,-Delmotte, V.,
609 Miller, H., Motoyama, H., Narita, H., Popp, T., Rasmussen, S.O., Raynaud, D.,
610 Rothlisberger, R., Ruth, U., Samyn, D., Schwander, J., Shoji, H.,
611 Siggard-Andersen, M.-L., Steffensen, J.P., Stocker, T., Sveinbjörnsdóttir, A.E.,
612 Svensson, A., Takata, M., Tison, J.-L., Thorsteinsson, Th., Watanabe, O.,
613 Wilhelms, F., and White, J.W.C.: High-resolution record of Northern Hemisphere
614 climate extending into the last interglacial period, Nature, 431, 147–151, 2004.
615 Beermann, F., Langer, M., Wetterich, S., Strauss, J., Boike, J., Fiencke, C.,
616 Schirrmeister, L., Pfeiffer, E.-M., and Kutzbach, L.: Permafrost thaw and release
617 of inorganic nitrogen from polygonal tundra soils in eastern Siberia,
618 Biogeosciences Discussions, https://doi.org/10.5194/bg-2016-117, 2016.
619 Bigelow, N.H., Brubaker, L.B., Edwards, M.E., Harrison, S.P., Prentice, I.C.,
620 Anderson, P.M., Andreev, A.A., Bartlein, P.J., Christensen, T.R., Cramer, W.,
621 Kaplan, J.O., Lozhkin, A.V., Matveyeva, N.V., Murray, D.F., McGuire, A.D.,
622 Razzhivin, V.Y., Ritchie, J.C., Smith, B., Walker, D.A., Gajewski, K., Wolf, V.,
623 Holmqvist, B.H., Igarashi, Y., Kremenetskii, K., Paus, A., Pisaric, M.F.J., and
624 Volkova, V.S.: Climate change and arctic ecosystems: 1. Vegetation changes north
625 of 55 °N between the last glacial maximum, mid-Holocene, and present, Journal of
626 Geophysical Research, 108, DOI: 10.1029/2002JD002558, 2008.
627 Binney, H.A., Edwards, M.E., Macias-Fauria, M., Lozhkin, A., Anderson, P., Kaplan,
628 J.O., Andreev, A.A., Bezrukova, E., Blyakharchuk, T., Jankovska, V., Khazina, I.,

Krivonogov, S., Kremenetski, K., Nield, J., Novenko, E., Ryabogina, N., Solovieva, N., Willis, K.J., and Zernitskaya, V.: Vegetation of Eurasia from the last glacial maximum to present: key biogeographic patterns, Quaternary Science Reviews, 157, 80–97, 2017.

Binney, H.A., Willis, K.J., Edwards, M.E., Bhagwat, S.A., Anderson, P.M., Andreev, A.A., Blaauw, M., Damblon, F., Haesaerts, P., Kienast, F., Kremenetski, K.V., Krivonogov, S.K., Lozhkin, A.V., MacDonald, G.M., Novenko, E.Y., Oksane, P., Sapelko, T.V., Väliranta, M., and Vazhenina, L.: The distribution of late-Quaternary woody taxa in northern Eurasia: evidence from a new macrofossil database, Quaternary Science Reviews, 28, 2445–2464, 2009.

Birks, H.J.B.: Estimating the amount of compositional change in late-Quaternary pollen-stratigraphical data, Vegetation History and Archaeobotany, 16, 197–202, 2007.

Biskaborn, B.K., Herzschuh, U., Bolshiyanov, D., Savelieva, L., and Diekmann, B.: Environmental variability in northeastern Siberia during the last ~13,300 yr inferred from lake diatoms and sediment-geochemical parameters, Palaeogeography, Palaeoclimatology, Palaeoecology, 329–330, 22–36, 2012.

Brewer, S., Cheddadi, R., de Beaulieu, J.L., Reille, M., and 154 data contributors: The spread of deciduous *Quercus* throughout Europe since the last glacial period, Forest Ecology and Management, 156, 27–48, 2002.

Broström, A.: Estimating source area of pollen and pollen productivity in the cultural landscapes of southern Sweden – developing a palynological tool for quantifying past plant cover, Quaternary Geology, Department of Geology, Lund University, 116 pp, 2002.

Broström, A., Sugita, S., and Gaillard, M.-J.: Pollen productivity estimates for the reconstruction of past vegetation cover in the cultural landscape of southern Sweden, The Holocene, 14, 368–381, 2004.

Brown, J., Ferrians, Jr., O.J., Heginbottom, J.A., and Melnikov, E.S.: Circum-Arctic map of permafrost and ground-ice conditions. Washington, DC: U.S. Geological Survey in Cooperation with the Circum-Pacific Council for Energy and Mineral

Resources, Circum-Pacific Map Series CP-45, scale 1:10,000,000, 1 sheet, 1997.

Bunting, M.J., Schofield, J.E., and Edwards, K.J.: Estimates of relative pollen productivity (RPP) for selected taxa from southern Greenland: A pragmatic solution, Review of Palaeobotany and Palynology, 190, 66–74, 2013.

Cao, X., Herzschuh, U., Ni, J., Zhao, Y., and Böhmer, T.: Spatial and temporal distributions of major tree taxa in eastern continental Asia during the last 22,000 years, The Holocene, 25, 79–91, 2015.

Cao, X., Ni, J., Herzschuh, U., Wang, Y., and Zhao, Y.: A late Quaternary pollen dataset in eastern continental Asia for vegetation and climate reconstructions: set-up and evaluation, Review of Palaeobotany and Palynology, 194, 21–37, 2013.

Cheng, H., Edwards, R.L, Sinha, A., Spötl, C., Yi, L., Chen, S., Kelly, M., Kathayat, G., Wang, X., Li, X., Kong, X., Wang, Y., Ning, Y., and Zhang, H.: The Asian monsoon over the past 640,000 years and ice age terminations, Nature, 534, 640–646, 2016.

Chen, F., Jia, J., Chen, J., Li, G., Zhang, X., Xie, H., Xia, D., Huang, W., and An, C.: A persistent Holocene wetting trend in arid central Asia, with wettest conditions in the late Holocene, revealed by multi-proxy analyses of loess-paleosol sequences in Xingjiang, China, Quaternary Science Reviews, 146, 134–146, 2016.

Chen, F., Yu, Z., Yang, M., Ito, E., Wang, S., Madsen, D.B., Huang, X., Zhao,Y., Sato, T., Birks, H.J.B., Boomer, I., Chen, J., An, C., and Wünnemann, B.: Holocene moisture evolution in arid central Asia and its out-of-phase relationship with Asian monsoon history, Quaternary Science Reviews, 27, 351–364, 2008.

Dulamsuren, C., Welk, E., Jäger, E.J., Hauck, M., and Mühlenberg, M.: Range-habitat relationships of vascular plant species at the taiga forest-steppe borderline in the western Khentey Mountains, northern Mongolia, Flora 200, 376–397, 2005.

Eisenhut, G.: Untersuchung über die Morphologie und Ökologie der Pollenkörner heimischer und fremdländischer Waldbäume, Parey, Hamburg, 1961.

Frost, G.V., and Epstein, H.E.: Tall shrub and tree expansion in Siberian tundra ecotones since the 1960s, Global Change Biology, 20, 1264–1277, 2014.

Fyfe, R.M., Twiddle, C., Sugita, S., Gaillard, M.-J., Barratt, P., Caseldine, C.J., Dodson, J., Edwards, K.J., Farrell, M., Froyd, C., Grant, M.J., Huckerby, E., Innes, J.B., Shaw, H., and Waller, M.: The Holocene vegetation cover of Britain and Ireland: overcoming problems of scale and discerning patterns of openness, Quaternary Science Reviews, 73, 132–148, 2013.

Gregory, P.H.: The microbiology of the atmosphere, 2nd ed., Leonard Hill, Aylesbury, 252 pp, 1973.

Guthrie, R.D.: New carbon dates link climatic change with human colonization and Pleistocene extinctions, Nature, 441, 207–209, 2006.

He, Y., Huang, J., Shugart, H.H., Guan, X., Wang, B., and Yu, K.: Unexpected evergreen expansion in the Siberia forest under warming hiatus, Journal of Climate, 30, 5021–5037, 2017.

Herzschuh, U., Birks, H.J.B., Laepple, T., Andreev, A., Melles, M., and Brigham-Grette, J.: Glacial legacies on interglacial vegetation at the Pliocene-Pleistocene transition in NE Asia, Nature Communications, 11967, DOI: 10.1038/ncomms11967, 2016.

Hong, B., Liu, C., Lin, Q., Yasuyuki, S., Leng, X., Wang, Y., Zhu, Y., and Hong, Y.: Temperature evolution from the $\delta^{18}O$ record of Hani peat, Northeast China, in the last 14000 years, Science in China Series D: Earth Science, 52, 952–964, 2009.

Hou, X.: Vegetation Atlas of China, Beijing: Science Press, 2001.

Intergovernmental Panel on Climate Change (IPCC): Climate change 2007: the physical science basis summary for policymakers, Geneva, Switzerland: World Meteorological Organization, 2007.

Isaev, A.P., Protopopov, A.V., Protopopova, V.V., Egorova, A.A., Timofeyev, P.A., Nikolaev, A.N., Shurduk, I.F., Lytkina, L.P., Ermakov, N.B., Nikitina, N.V., Efimova, A.P., Zakharova, V.I., Cherosov, M.M., Nikolin, E.G., Sosina, N.K., Troeva, E.I., Gogoleva, P.A., Kuznetsova, L.V., Pestryakov, B.N., Mironova, S. I., and Sleptsova, N.P.: Vegetation of Yakutia: Elements of Ecology and Plant Sociology, in: The Far North, vol. 3, edited by: Troeva, E.I., Isaev, A.P., Cherosov, M.M., and Karpov, N.S., Springer Netherlands, Dordrecht, 143–260, 2010.

719 Jackson, S.T., Overpeck, J.T., Webb, T., Keattch, S.E., and Anderson, K.H.: Mapped
720 plant-macrofossil and pollen records of late Quaternary vegetation change in
721 eastern North America, Quaternary Science Reviews, 16, 1–70, 1997.
722 Jin, L., Chen, F., Morrill, C., Otto-Bliesner, B.L., and Rosenbloom, N.: Causes of
723 early Holocene desertification in arid central Asia, Climate Dynamics, 38, 1577–
724 1591, 2012.
725 Jørgensen, T., Haile, J., Möller, P., Andreev, A., Boessenkool, S., Rasmussen, M.,
726 Kienast, F., Coissac, E., Taberlet, P., Brochmann, C., Bigelow, N.H., Andersen, K.,
727 Orlando, L., Gilbert, M.T.P., and Willerslev, E.: A comparative study of ancient
728 sedimentary DNA, pollen and macrofossils from permafrost sediments of
729 northern Siberia reveals long-term vegetational stability, Molecular Ecology, 21,
730 1989–2003, 2012.
731 Juggins, S.: rioja: Analysis of Quaternary Science Data. version 0.9-15.1, Available at:
732 http://cran.r-project.org/web/packages/rioja/index.html, 2018.
733 Katamura, F., Fukuda, M., Bosikov, N.P., and Desyatkin, R.V.: Forest fires and
734 vegetation during the Holocene in central Yakutia, eastern Siberia, Journal of
735 Forest Research, 14, 30–36, 2009.
736 Kharuk, V.I., Ranson, K.J., Dvinskaya, M.L., and Im, S.: Siberian pine and larch
737 response to climate warming in the southern Siberian mountain forest: tundra
738 ecotone. In: Balzter, H. (eds) Environmental Change in Siberia, Springer
739 Netherlands, 40, 115–132, 2010.
740 Kirdyanov, A.V., Hagedorn, F., Knorre, A.A., Fedotova, E.V., Vaganov, E.A.,
741 Naurzbaev, M.M., Moiseev, P.A., and Rigling, A.: 20th century tree-line advance
742 and vegetation changes along an altitudinal transect in the Putorana Mountains,
743 northern Siberia, Boreas, 41, 56–67, 2012.
744 Klemm, J., Herzschuh, U., and Pestryakova, L.A.: Vegetation, climate and lake
745 changes over the last 7000 years at the boreal treeline in north-central Siberia,
746 Quaternary Science Reviews, 147, 422–434, 2016.
747 Kruse, S., Wieczorek, M., Jeltsch, F., and Herzschuh, U.: Treeline dynamics in Siberia
748 under changing climates as inferred from an individual-based model for *Larix*,

749 Ecological Modelling, 338, 101–121, 2016.
750 Laskar, J., Robutel, P., Joutel, F., Gastineau, M., Correia, A.C.M., and Levrard, B.: A
751 long-term numerical solution for the insolation quantities of the Earth, Astronomy
752 and Astrophysics, 428, 261–285, 2004.
753 Li, F.: Pollen productivity estimates and pollen-based reconstructions of Holocene
754 vegetation cover in northern and temperate China for climate modelling, PhD
755 thesis, Linnaeus University, 2016.
756 Li, F., Gaillard, M.-J., Sugita, S., Mazier, F., Xu, Q., Zhou, Z., Zhang, Y., Li, Y., and
757 Laffly, D.: Relative pollen productivity estimates for major plant taxa of cultural
758 landscapes in central eastern China, Vegetation History and Archaeobotany, 26,
759 587–605, 2017.
760 Li, J., Fan, K., and Zhou, L.: Satellite observations of El Niño impacts on Eurasian
761 spring vegetation greenness during the period 1982–2015, Remote Sensing, 9,
762 628, 2017.
763 Li, Y., Nielsen, A.B., Zhao, X., Shan, L., Wang, S., Wu, J., and Zhou, L.: Pollen
764 production estimates (PPEs) and fall speeds for major tree taxa and relevant
765 source areas of pollen (RSAP) in Changbai Mountain, northeastern China,
766 Review of Palaeobotany and Palynology, 216, 92–100, 2015.
767 Liu, Z., Wen, X., Brady, E.C., Otto-Bliesner, B., Yu, G., Lu, H., Cheng, H., Wang, Y.,
768 Zheng, W., Ding, Y., Edwards, R.L., Cheng, J., Liu, W., and Yang, H.: Chinese
769 cave records and the East Asia Summer Monsoon, Quaternary Science Reviews,
770 83, 115–128, 2014.
771 Lloyd, A.H., Bunn, A.G., and Berner, L.: A latitudinal gradient in tree growth response
772 to climate warming in the Siberian taiga, Global Change Biology, 17, 1935–1945,
773 2010.
774 Ma, Y., Liu, K., Feng, Z., Sang, Y., Wang, W., and Sun, A.: A survey of modern pollen
775 and vegetation along a south–north transect in Mongolia, Journal of Biogeography,
776 35, 1512–1532, 2008.
777 MacDonald, G.M., Kremenetski, K.V., and Beilman, D.W.: Climate change and the
778 northern Russian treeline zone, Philosophical Transactions of the Royal Society,

363, 2285–2299, 2008.

MacDonald, G.M.,Velichko, A.A., Kremenetski, C.V., Borisova, O.K., Goleva, A.A., Andreev, A.A., Cwynar, L.C., Riding, R.T., Forman, S.L., Edwards, T.W.D., Aravena, R., Hammarlund, D., Szeicz, J.M., and Gattaulin, V.N.: Holocene treeline history and climate change across northern Eurasia, Quaternary Research, 53, 302–311, 2000.

Marcott, S.A., Shakun, J.D., Clark, P.U., and Mix, A.C.: A reconstruction of regional and global temperature for the past 11,300 years, Science, 339, 1198–1201, 2013.

Marquer, L., Gaillard, M.J., Sugita, S., Trondman, A.K., Mazier, F., Nielsen, A.B., Fyfe, R.M., Odgaard, B.V., Alenius, T., Birks, H.J.B, Bjune, A.E., Christiansen, J., Dodson, J., Edwards, K.J., Giesecke, T., Herzschuh, U., Kangur, M., Lorenz, S., Poska, A., Schult, M., and Seppä, H.: Holocene changes in vegetation composition in northern Europe: why quantitative pollen-based vegetation reconstructions matter, Quaternary Science Reviews, 90, 199–216, 2014.

Marquer, L., Gaillard, M.-J., Sugita, S., Poska, A., Trondman, A.-K., Mazier, F., Nielsen, A.B., Fyfe, R.M., Jönsson, A.M., Smith, B., Kaplan, J.O., Alenius, T., Birks, H.J.B., Bjune, A.E., Christiansen, J., Dodson, J., Edwards, K.J., Giesecke, T., Herzschuh, U., Kangur, M., Koff, T., Latałowa, M., Lechterbeck, J., Olofsson, J., and Seppä, H.: Quantifying the effects of land use and climate on Holocene vegetation in Europe, Quaternary Science Reviews, 171, 20-37, 2017.

Mazier, F., Gaillard, M.-J., Kuneš, P., Trodmann, A.-K., and Broström, A.: Testing the effect of site selection and parameter setting on REVEALS-model estimates of plant abundance using the Czech Quaternary Palynological Database, Review of Palaeobotany and Palynology, 187, 38–49, 2012.

Miller, G.H., Alley, R., Brigham-Grette, J., Fitzpatrick, J.J., Polyak, L., Serreze, M.C., and White, J.W.C.: Arctic amplification: can the past constrain the future? Quaternary Science Reviews, 29, 1779–1790, 2010.

Moiseev, P.A.: Climate-change impacts on radial growth and formation of the age structure of highland larch forests in Kuznetsky Alatau, Russian Journal of Ecology, 1, 10–16, 2002.

809 Monserud, R.A., Denissenko, O.V., and Tchebakova, N.M.: Comparison of Siberian
810 paleovegetation to current and future vegetation under climate change, Climate
811 Research, 3, 143–159, 1993.
812 Nazarova, L., Lüpfert, H., Subetto, D., Pestryakova, L., and Diekmann, B.: Holocene
813 climate conditions in central Yakutia (Eastern Siberia) inferred from sediment
814 composition and fossil chironomids of Lake Temje, Quaternary International,
815 290–291, 264–274, 2013.
816 Ni, J., Yu, G., Harrison, S.P., and Prentice, I.C.: Palaeovegetation in China during the
817 late Quaternary: biome reconstructions based on a global scheme of plant
818 functional types, Palaeogeography, Palaeoclimatology, Palaeoecology, 289, 44–61,
819 2010.
820 Nielsen, A.B., Giesecke, T., Theuerkauf, M., Feeser, I., Behre, K.-E., Beug, H.-J.,
821 Chen, S.-H., Christiansen, J., Dörfler, W., Endtmann, E., Jahns, S., de Klerk, P.,
822 Kühl, N., Latałowa, M., Odgaard, B.V., Rasmussen, P., Stockholm, J.R., Voigt, R.,
823 Wiethold, J., and Wolters, S.: Quantitative reconstructions of changes in regional
824 openness in north-central Europe reveal new insights into old questions,
825 Quaternary Science Reviews, 47, 131–149, 2012.
826 Niemeyer, B., Klemm, J., Pestryakova, J.A., and Herzschuh, U.: Relative pollen
827 productivity estimates for common taxa of the northern Siberian Arctic, Review
828 of Palaeobotany and Palynology, 221, 71–82, 2015.
829 Osawa, A., Zyryanova, O. A., Matsuura, Y., Kajimoto, T., and Wein, R. W.:
830 Permafrost Ecosystems: Siberian Larch Forests, Springer, Auflage, 502, 2010.
831 Pailler, D., and Bard, E.: High frequency paleoceanographic changes during the past
832 140,000 years recorded by the organic matter in sediments off the Iberian Margin,
833 Palaeogeography, Palaeoclimatology, Palaeoecology, 181, 431–452, 2002.
834 Parsons, R.W., and Prentice, I.C.: Statistical approaches to R-values and the pollen–
835 vegetation relationship, Review of Palaeobotany and Palynology, 32, 127–152,
836 1981.
837 Pearson, R.G., Phillips, S.J., Loranty, M.M., Beck, P.S.A., Damoulas, T., Knight, S.J.,
838 and Goetz, S.J.: Shifts in arctic vegetation and associated feedbacks under climate

change, Nature Climate Change, 3, 673–677, 2013.

Pelánková, B., Kuneš, P., Chytrý, M., Jankovská, V., Ermakov, N., and Svobodová-Svitavská, H.: The relationship of modern pollen spectra to vegetation and climate along a steppe-forest-tundra transition in southern Siberia, explored by decision trees, The Holocene, 18, 1259–1271, 2008.

Pisaric, M.F.J., MacDonald, G.M., Cwynar, L.C., and Velichko, A.A.: Modern pollen and conifer stomates from north-central Siberian lake sediments: their use in interpreting late Quaternary fossil pollen assemblages, Arctic, Antarctic, and Alpine Research, 33, 19–27, 2001.

Prentice, I.C.: Pollen representation, source area, and basin size: toward a unified theory of pollen analysis, Quaternary Research, 23, 76–86, 1985.

Prentice, I.C., and Parsons, R.W.: Maximum likelihood linear calibration of pollen spectra in terms of forest composition, Biometrics, 39, 1051–1057, 1983.

R Core Team: R: A Language and Environment for Statistical Computing, R Foundation for Statistical Computing, Vienna, 2017.

Ren, G., 2007. Changes in forest cover in China during the Holocene. Vegetation History and Archaeobotany, 16, 119–126.

Sarda-Espinosa, A.: dtwclust: Time series clustering along with optimizations for the dynamic time warping distance, version 5.2.0, Available at: http://cran.r-project.org/web/packages/dtwclust/index.html, 2018.

Schuur, E.A.G., Vogel, J.G., Crummer, K.G., Lee, H., Sickman, J.O., and Osterkamp, T.E.: The effect of permafrost thaw on old carbon release and net carbon exchange from tundra, Nature, 459, 556–559, 2009.

Serreze, M.C., Walsh, J.E., Chapin III, F.S., Osterkamp, T., Dyurgerov, M., Romanovsky, V., Oechel, W.C., Morison, J., Zhang, T., and Barry, R.G.: Observational evidence of recent change in the northern high-latitude environment, Climatic Change, 46, 159–207, 2000.

Shestakova, T.A., Voltas, J., Saurer, M., Siegwolf, R.T.W., and Kirdyanov, A.V.: Warming effects on *Pinus sylvestris* in the cold-dry Siberian forest-steppe: positive or negative balance of trade? Forests, 8, 490, doi: 10.3390/f8120490.,

2017.

Soja, A.J., Tchebakova, N.M., French, N.H.F., Flannigan, M.D., Shugart, H.H., Stocks, B.J., Sukhinin, A.I., Parfenova, E.I., Chapin III, F.S., and Stackhouse Jr, P.W.: Climate-induced boreal forest change: predictions versus current observations, Global and Planetary Change, 56, 274–296, 2007.

Stuart, A., and Ord, J.K.: Kendall's Advanced Theory of Statistic. Volume 1: Distribution Theory, Edward Arnold, London, 1994.

Sugita, S.: A model of pollen source area for an entire lake surface, Quaternary Research, 39, 239–244, 1993.

Sugita, S.: Pollen representation of vegetation in Quaternary sediments: theory and method in patchy vegetation, Journal of Ecology, 82, 881–897, 1994.

Sugita, S.: Theory of quantitative reconstruction of vegetation I: pollen from large sites REVEALS regional vegetation composition, The Holocene, 17, 229–241, 2007.

Sugita, S., Gaillard, M.-J., and Broström, A.: Landscape openness and pollen records: a simulation approach, The Holocene, 9, 409–421, 1999.

Sugita, S., Parshall, T., Calcote, R., and Walker, K.: Testing the landscape reconstruction algorithm for spatially explicit reconstruction of vegetation in northern Michigan and Wisconsin, Quaternary Research, 74, 289–300, 2010.

Swann, G.E.A., Mackay, A.W., Leng, M.J., and Demory, F.: Climate change in Central Asia during MIS 3/2: a case study using biological responses from Lake Baikal, Global and Planetary Change, 46, 235–253, 2005.

Swann, G.E.A., Leng, M.J., Juschus, O., Melles, M., Brigham-Grette, J., and Sloane, H.J.: A combined oxygen and silicon diatom isotope record of Late Quaternary change in Lake El'gygytgyn, North East Siberia, Quaternary Science Reviews, 29, 774–786, 2010.

Tarasov, P.E., Williams, J.W., Andreev, A.A., Nakagawa, T., Bezrukova, E., Herzschuh, U., Igarashi, Y., Müller, S., Werner, K., and Zheng, Z.: Satellite- and pollen-based quantitative woody cover reconstructions for northern Asia: Verification and application to late-Quaternary pollen data, Earth and Planetary

Science Letters, 264, 284–298, 2007.

Tarasov, P.E., Volkova, V.S., Webb, T., Guiot, J., Andreev, A.A., Bezusko, L.G., Bezusko, T.V., Bykova, G.V., Dorofeyuk, N.I., Kvavadze, E.V., Osipova, I.M., Panova, N.K., and Sevastyanov, D.V.: Last glacial maximum biomes reconstructed from pollen and plant macrofossil data from northern Eurasia, Journal of Biogeography, 27, 609–620, 2000.

Tarasov, P.E., Webb, T., Andreev, A.A, Afanas'Eva, N.B., Berezina, N.A., Bezusko, L.G., Blyakharchuk, T.A., Bolikhovskaya, N.S., Cheddadi, R., Chernavskaya, M.M., Chernova, G.M., Dorofeyuk, N.I., Dirksen, V.G., Elina, G.A., Filimonova, L.V., Glebov, F.Z., Guiot, J., Gunova, V.S., Harrison, S.P., Jolly, D., Khomutova, V.I., Kvavadze, E.V., Osipova, I.M., Panova, N.K., Prentice, I.C., Saarse, L., Sevastyanov, D.V., Volkova, V.S., and Zernitskaya, V.P.: Present-day and mid-Holocene biomes reconstructed from pollen and plant macrofossil data from the Former Soviet Union and Mongolia, Journal of Biogeography, 25, 1029–1053, 1998.

Tchebakova, N.M., Parfenova, E., and Soja, A.J.: The effects of climate, permafrost and fire on vegetation change in Siberia in a changing climate, Environmental Research Letters, 4, 045013. doi:10.1088/1748-9326/4/4/045013, 2009.

Tchebakova, N.M., Rehfeldt, G., and Parfenova, E.I.: Impacts of climate change on the distribution of *Larix* spp. and *Pinus sylvestris* and their climatypes in Siberia, Mitigation and Adaptation Strategies for Global Change, 11, 861–882, 2005.

ter Braak, C.J.F.: Canonical correspondence analysis: a new eigenvector technique for multivariate direct gradient analysis, Ecology, 67, 1167–1179, 1986.

ter Braak, C.J.F., and Šmilauer, P.: CANOCO reference manual and CanoDraw for Windows user's guide: software for canonical community ordination (version 4.5), Microcomputer Power, 2002.

Tian, F., Cao, X., Dallmeyer, A., Lohmann, G., Zhang, X., Ni, J., Andreev, A.A., Anderson, P.M., Lozhkin, A.V., Bezrukova, E., Rudaya, N., Xu, Q., and Herzschuh, U.: Biome changes and their inferred climatic drivers in northern and eastern continental Asia at selected times since 40 cal ka BP, Vegetation History

and Archaeobotany, 27: 365–379, 2018.

Trondman, A.-K., Gaillard, M.-J., Mazier, F., Sugita, S., Fyfe, R.M., Nielsen, A.B., Twiddle, C., Barratt, P., Birks, H.J.B., Bjune, A.E., Björkman, L., Broström, A., Caseldine, C., David, R., Dodson, J., Dörfler, W., Fischer, E., van Geel, B., Giesecke, T., Hultberg, T., Kalnina, L., Kangur, M., van der Knaap, W.O., Koff, T., Kuneš, P., Lagerås, P., Latałowa, M., Lechterbeck, J., Leroyer, C., Leydet, M., Lindbladh, M., Marquer, L., Mitchell, F.J.G., Odgaard, B.V., Peglar, S.M., Persoon, T., Poska, A., Rösch, M., Seppä, H., Veski, S., and Wick, L.: Pollen-based quantitative reconstruction of Holocene regional vegetation cover (plant-functional types and land-cover types) in Europe suitable for climate modelling, Global Change Biology, 21, 676–697, 2015.

Trondman, A.-K., Gaillard, M.-J., Sugita, S., Björkman, L., Greisamn, A., Hultberg, T., Lagerås, P., Lindbladh, M., and Mazier, F.: Are pollen records from small sites appropriate for REVEALS model-based quantitative reconstructions of past regional vegetation? An empirical test in southern Sweden, Vegetation History and Archaeobotany, 25, 131–151, 2016.

Tseplyayev, V.P.: The forests of the U.S.S.R.: an economic characterisation, Lesa SSSR, Moscow, 1961.

Tzedakis, P.C., and Bennett, K.D.: Interglacial vegetation succession: a view from southern Europe, Quaternary Science Reviews, 14, 967–982, 1995.

Vandenberghe, J., French, H.M., Gorbunov, A., Marchenko, S., Velichko, A.A., Jin, H., Cui, Z., Zhang, T., and Wan, X.: The Last Permafrost Maximum (LPM) map of the Northern Hemisphere: permafrost extent and mean annual air temperatures, 25–17 ka BP, Boreas, 43, 652–666, 2014.

Wang, Y., and Herzschuh, U.: Reassessment of Holocene vegetation change on the upper Tibetan Plateau using the pollen-based REVEALS model, Review of Palaeobotany and Palynology, 168, 31–40, 2011.

Wieczorek, M., Kruse, S., Epp, L.S., Kolmogorov, A., Nikolaev, A.N., Heinrich, I., Jeltsch, F., Pestryakova, L.A., Zibulski, R., and Herzschuh, U.: Dissimilar responses of larch stands in northern Siberia to increasing temperatures—a field

and simulation based study, Ecology, 98, 2343–2355, 2017.

Willerslev, E., Davison, J., Moora, M., Zobel, M., Coissac, E., Edwards, M.E., Lorenzen, E.D., Vestergård, M., Gussarova, G., Haile, J., Craine, J., Gielly, L., Boessenkool, S., Epp, L.S., Pearman, P.B., Cheddadi, R., Murray, D., Bråthen, K.A., Yoccoz, N., Binney, H., Cruaud, C., Wincker, P., Goslar, T., Alsos, I.G., Bellemain, E., Brysting, A.K., Elven, R., Sønstebø, J.H., Murton, J., Sher, A., Rasmussen, M., Rønn, R., Mourier, T., Cooper, A., Austin, J., Möller, P., Froese, D., Zazula, G., Pompanon, F., Rioux, D., Niderkorn, V., Tikhonov, A., Savvinov, G., Roberts, R.G., MacPhee, R.D.E., Gilbert, M.T.P., Kjær, K.H., Orlando, L., Brochmann, C., and Taberlet, P.: Fifty thousand years of Arctic vegetation and megafaunal diet, Nature, 506, 47–51, 2014.

Xie, H., Zhang, H., Ma, J., Li, G., Wang, Q., Rao, Z., Huang, W., Huang, X., and Chen, F.: Trend of increasing Holocene summer precipitation in arid central Asia: Evidence from an organic carbon isotopic record from the LJW10 loess section in Xinjiang, NW China, Palaeogeography, Palaeoclimatology, Palaeoecology, DOI: 10.1016/j.palaeo.2018.04.006, 2018.

Xu, Q., Cao, X., Tian, F., Zhang, S., Li, Y., Li, M., Liu, Y., and Liang, J.: Relative pollen productivities of typical steppe species in northern China and their potential in past vegetation reconstruction, Science China: Earth Sciences, 57, 1254–1266, 2014.

Zhang, N., Yasunari, T., and Ohta, T.: Dynamics of the larch taiga permafrost coupled system in Siberia under climate change, Environmental Research Letters, 6, 24003–24006, 2011.

Zimov, S.A., Chuprynin, V.I., Oreshko, A.P., Chapin III, F.S., Reynolds, J.F., and Chapin, M.C.: Steppe-tundra transition: an herbivore-driven biome shift at the end of the Pleistocene, The American Naturalist, 146, 765–794, 1995.

Zimov, S.A., Zimov, N.S., Tikhonov, A.N., and Chapin III, F.S.: Mammoth steppe: a high-productivity phenomenon, Quaternary Science Reviews, 57, 26–45, 2012.

Appendices

Appendix 1 Distribution of the 203 fossil pollen sites together with the modern permafrost extent in northern Asia. The number of each site is used as its site ID in Appendix 2.

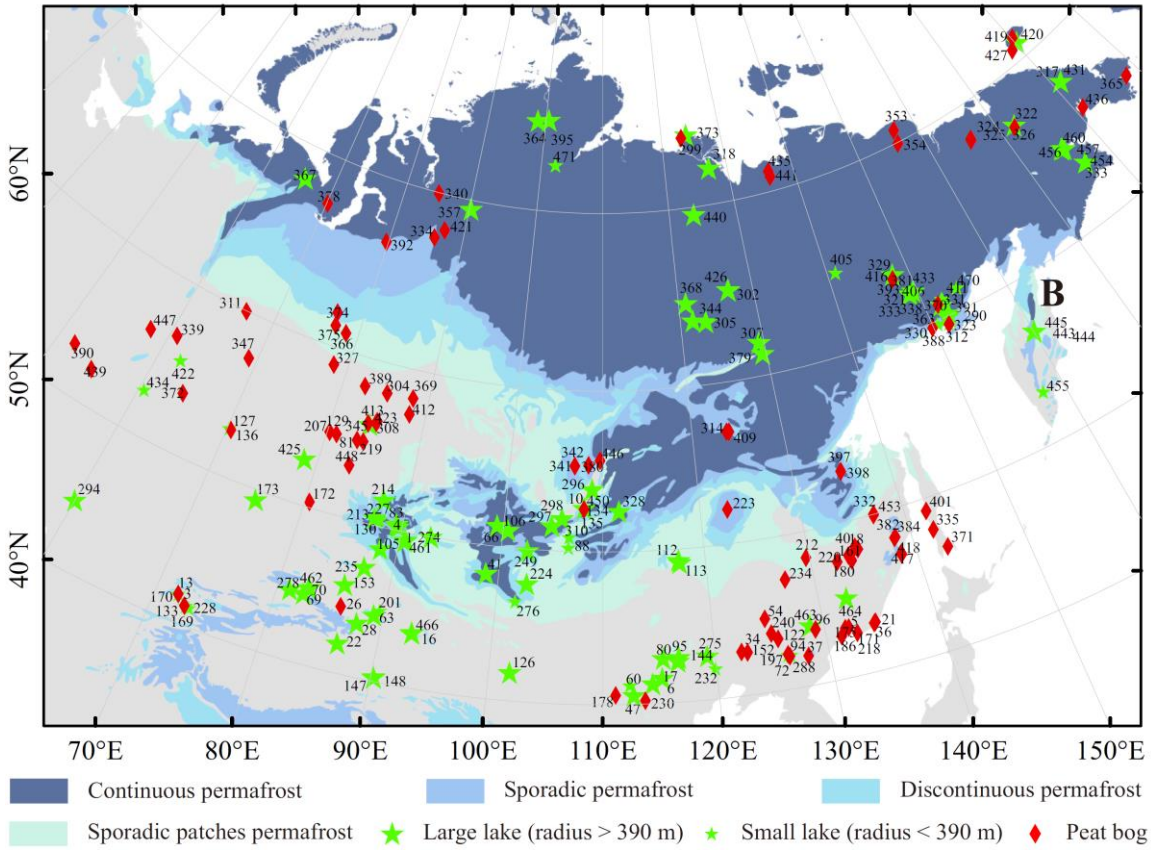

992 **Appendix 2** Metadata for all pollen records used in this study. Original publications list see https://doi.pangaea.de/10.1594/PANGAEA.898616.

Group	Site ID	Site	Lat.	Long.	Elev. (m)	Basin type	Pollen count	Area (ha)	Radius (m)	Dating method	Num. of dating	Time span (cal ka BP)	Resol. (year)	Reference
G1	294	Aral Lake	44.42	59.98	53	Lake	Yes	330000	32410	^{14}C	4U	8.7-0	260	Aleshinskaya, Z.V. unpublished.
G2	372	Mokhovoye	53.77	64.25	178	Bog	Yes	20	252	^{14}C	4C+1E	6.0-0	180	Kremenetskii et al., 1994
G2	439	Novienky peat bog	52.24	54.75	197	Bog	Yes	-	-	^{14}C	1U	4.5-0	270	López-García et al., 2003
G2	422	Zaboinoe Lake	55.53	62.37	275	Lake	Yes	6	138	^{14}C	1U	12.3-0.1	220	Khomutova and Pushenko, 1995
G2	434	Lake Fernsehsee	52.83	60.50	290	Lake	Yes	0	38	^{14}C	10A	9.1-0.4	220	Stobbe et al., 2015
G2	390	Pobochnoye	53.03	51.84	81	Bog	No	79	500	^{14}C	10C+6E	14.4-0	540	Kremenetski et al., 1999
G3	311	Chesnok Peat	60.00	66.50	42	Bog	Yes	-	-	^{14}C	7C	10.6-0.5	280	Volkova, 1966
G3	347	Komaritsa Peat	57.50	69.00	42	Bog	Yes	-	-	^{14}C	10C	10.5-0.5	350	Volkova, 1966
G3	447	UstMashevskoe	56.32	57.88	220	Bog	Yes	30	309	^{14}C	5C	7.8-0	150	Panova et al., 1996
G3	339	Karasieozerskoe	56.77	60.75	230	Bog	Yes	914	1706	^{14}C	3A	5.9-0.1	190	Panova, 1997
G4	378	Nulsaveito	67.53	70.17	57	Bog	Yes	-	-	^{14}C	4A+1C	8.4-6.4	70	Panova, 1990
G4	367	Lyadhej-To Lake	68.25	65.75	150	Lake	Yes	197	792	^{14}C	14A+6E	12.5-0.3	170	Andreev et al., 2005
G5	169	Nizhnee Lake	41.30	72.95	1371	Lake	No	-	70	^{14}C	4E	1.5-0	100	Beer et al., 2008
G5	228	Verkhnee Lake	41.30	72.95	1440	Lake	No	1	60	^{14}C	5E	1.5-0	100	Beer et al., 2008
G5	3	Ak Terk Lake	41.28	72.83	1748	Bog	No	-	-	^{14}C	2A	7.5-0	200	Beer et al., 2008
G5	133	Kosh Sas	41.85	71.97	1786	Bog	No	-	-	^{14}C	1A	3.5-0	100	Beer et al., 2008
G5	170	Ortok Lake	41.23	73.25	1786	Lake	No	-	60	^{14}C	5A	1-0	100	Beer et al., 2008
G5	13	Bakaly Lake	41.87	71.97	1879	Lake	No	1	50	^{14}C	4A	7-0	195	Beer et al., 2008
G6	425	Big Yarovoe Lake	52.85	78.63	79	Lake	Yes	6362	4500	inclination	-	4.3-0	190	Rudaya et al., 2012

										with Biwa	Lake			
G6	172	Ozerki	50.40	80.47	210	Bog	Yes	-	-	^{14}C	3A+13C	14.5-0	300	Tarasov et al., 1997
G6	127	Karas'e Lake	53.03	70.22	435	Lake	Yes	17	235	^{14}C	6U	5.5-0	170	Tarasov and Kremenetskii. 1995
G6	136	Kotyrkol	52.97	70.42	439	Bog	Yes	-	-	^{14}C	8U	4.5-0.5	180	Tarasov and Kremenetskii. 1995
G6	173	Pashennoe Lake	49.37	75.40	871	Lake	Yes	64	451	^{14}C	5D+5E	9.5-0	280	Tarasov and Kremenetskii. 1995
G7	81	Gladkoye Bog	55.00	83.33	80	Bog	Yes	-	-	^{14}C	13C	11-0.5	170	Firsov et al., 1982
G7	308	Chaginskoe Mire	56.45	84.88	80	Bog	Yes	10	175	^{14}C	2C	8.8-0	320	Blyakharchuk, 2003.
G7	345	Kirek Lake	56.10	84.22	90	Lake	Yes	52	407	^{14}C	3G	10.5-1.5	190	Blyakharchuk, 2003
G7	413	Tom' River Peat	56.17	84.00	100	Bog	Yes	-	-	^{14}C	6C	10.1-0.2	390	Arkhipov and Votakh, 1980
G7	423	Zhukovskoye mire	56.33	84.83	106	Bog	Yes	-	-	^{14}C	9C+6H	11.2-0	130	Borisova et al., 2011
G7	219	Tolmachevsko	55.00	84.00	110	Bog	Yes	-	-	^{14}C	1A+3C	13-1.5	400	Volkov and Arkhipov, 1978
G7	207	Suminskoye	55.00	80.25	135	Bog	Yes	-	-	^{14}C	8A	3-0	200	Klimanov, 1976
G7	129	Kayakskoye	55.00	81.00	150	Bog	Yes	-	-	^{14}C	5C	6.5-0	210	Levina et al., 1987
G7	448	Kalistratikha	53.33	83.25	190	Bog	Yes	-	-	^{14}C	4A	39.0-12.7	1870	Zudin and Votakh, 1977
G8	389	Petropavlovka	58.33	82.50	100	Bog	Yes	-	-	^{14}C	4C+1E	10.5-0.1	160	Blyakharchuk, 1989
G8	304	Bugristoe	58.25	85.17	130	Bog	Yes	-	-	LSC	4C+1E	11.5-5.0	100	Blyakharchuk, 1989
G8	369	Maksimkin Yar	58.33	88.17	150	Bog	Yes	-	-	^{14}C	4C	8.3-0.2	170	Blyakharchuk, 1989
G8	412	Teguldet	57.33	88.17	150	Bog	Yes	-	-	LSC	3C	7.3-2.4	90	Blyakharchuk, 1989
G9	374	Nizhnevartovsk	62.00	76.67	54	Bog	Yes	-	-	^{14}C	3A+7C	11.1-0	300	Neustadt and Zelikson,

														1985
G9	375	Nizhnevartovskoye	61.25	77.00	55	Bog	Yes	-	-	^{14}C	1A+12C+1E	12.6-0	380	Neishtadt, 1976
G9	327	Entarnoye Peat	59.00	78.33	65	Bog	Yes	-	-	^{14}C	5C	14.9-0.9	460	Neishtadt, 1976
G9	366	Lukaschin Yar	61.00	78.50	65	Bog	Yes	-	-	^{14}C	13C	10.9-0.3	430	Neishtadt, 1976
G10	334	Igarka Peat	67.67	86.00	45	Bog	Yes	244	881	^{14}C	1A+2C	10.9-5.9	230	Kats, 1953
G10	392	Pur-Taz Peatland	66.70	79.73	50	Bog	Yes	5	126	^{14}C	5A	10.3-4.7	80	Peteet et al., 1998
G10	340	Karginskii Cape	70.00	85.00	60	Bog	Yes	-	-	^{14}C	13C	8.9-3.5	290	Firsov et al., 1972
G10	421	Yenisei	68.17	87.15	68	Bog	No	-	-	^{14}C	7C	6.5-1.6	110	Andreev and Klimanov 2000
G10	357	Lake Lama	69.53	90.20	77	Lake	Yes	64245	14300	^{14}C	26A+4D+4E	19.5-0	170	Andreev et al., 2004
G11	471	11-CH-12A Lake	72.40	102.29	60	Lake	Yes	3	100	^{14}C+Pb/Cs	8A+7E	7.0-0.1	110	Klemm et al., 2015
G11	364	Levinson-Lessing Lake	74.47	98.64	26	Lake	Yes	2145	2613	^{14}C	29A+1B+19E	35.3-0	390	Andreev et al., 2003
G11	395	SAO1	74.55	100.53	32	Lake	Yes	456000	38098	^{14}C	6A+5C	57.9-0	1320	Andreev et al., 2003
G12	462	Aibi Lake	45.02	82.83	200	Lake	Yes	100885	17920	^{14}C	8E	12.6-0	65	Wang et al., 2013
G12	69	Ebinur Lake	44.55	82.45	212	Lake	Yes	46421	12156	^{14}C	7U	13-0	900	Wen and Qiao, 1990
G12	70	Ebinur Lake_SW	45.00	82.80	212	Lake	Yes	46421	12156	^{14}C	6U	8.5-1.5	780	Lin, 1994
G12	26	Caotanhu Lake	44.42	86.02	380	Bog	Yes	2760	2964	^{14}C	5C	8.5-0	150	Zhang Y. et al., 2008
G12	63	Dongdaohaizi Lake	44.70	89.56	430	Lake	Yes	20	252	^{14}C	8U	5.5-0	85	Yan et al., 2004
G12	201	Sichanghu Lake	44.31	89.14	589	Lake	Yes	2000	2523	^{14}C	4U	1-0	50	Zhang Y. et al., 2004b
G12	22	Bosten Lake	41.97	86.55	1050	Lake	No	96608	17536	^{14}C	5U	13-0	420	Xu, 1998
G12	28	Chaiwopu Lake	43.55	87.78	1100	Lake	No	3101	3142	^{14}C	2U	10-0	845	Li and Yan, 1990
G12	278	Sayram Lake	44.57	81.15	2072	Lake	Yes	45800	12074	^{14}C	12E	13.8-0.1	90	Jiang et al., 2013
G13	153	Manas Lake	45.83	85.92	251	Lake	Yes	55000	13231	^{14}C	7C	13.5-1	210	Sun et al., 1994
G13	235	Wulungu Lake	47.22	87.30	479	Lake	Yes	67019	430	^{14}C+Pb/Cs	1C	9-0	80	Liu X.Q. et al., 2008

G14	214	Teletskoye Lake	51.72	87.65	1900	Lake	Yes	16610	7271	^{14}C+Pb/Cs	6E	1-0	20	Andreev et al., 2007
G14	227	Uzunkol Lake	50.48	87.11	1985	Lake	No	123	625	^{14}C	2A	17.5-0	210	Blyakharchuk et al., 2004
G14	130	Kendegelukol Lake	50.51	87.64	2050	Lake	No	5	130	^{14}C	7E	16-1	260	Blyakharchuk et al., 2004
G14	105	Hoton Nur Lake	48.62	88.35	2083	Lake	Yes	5021	3998	^{14}C	4A	6-0	60	Rudaya et al., 2009
G14	213	Tashkol Lake	50.45	87.67	2150	Lake	No	-	150	^{14}C	3C	16-3	250	Blyakharchuk et al., 2004
G14	4	Akkol Lake	50.25	89.63	2204	Lake	No	388	1111	^{14}C	12E	13.5-0	250	Blyakharchuk et al., 2007
G14	83	Grusha Lake	50.38	89.42	2413	Lake	No	130	644	^{14}C	3A+13E	14-1.5	250	Blyakharchuk et al., 2007
G15	274	Bayan Nuur	50.00	93.00	932	Lake	No	2968	3073	^{14}C	7E	15.7-0.2	210	Krengel, 2000
G15	1	Achit Nur Lake	49.50	90.60	1435	Lake	No	29700	9723	^{14}C	4E	14-0.5	700	Gunin et al., 1999
G15	461	Achit Nuur	49.42	90.52	1444	Lake	No	29700	9723	^{14}C	10E	20.2-0	250	Sun et al., 2013
G16	148	Lop Nur_1998	40.28	90.25	780	Lake	No	535000	41267	^{14}C	3U	22-2	2000	Yan et al., 1998
G16	147	Lop Nur_1983	40.33	90.25	800	Lake	Yes	535000	41267	^{14}C	3U	22-0.5	1600	Yan et al., 1983
G16	16	Barkol Lake	43.62	92.80	1575	Lake	Yes	11300	5997	^{14}C	1A+10E	10-0	115	Tao et al., 2009
G16	466	Balikun Lake	43.68	92.80	1575	Lake	Yes	7897	5014	^{14}C	1D+5E	30.5-9	250	An et al., 2013
G17	126	Juyan Lake	41.89	101.85	892	Lake	Yes	72000	15139	^{14}C	5E	10.5-1.5	140	Herzschuh et al., 2004
G18	88	Gun Nur Lake	50.25	106.60	600	Lake	No	33	325	^{14}C	7E	11-0	320	Gunin et al., 1999
G18	249	Yamant Nur Lake	49.90	102.60	1000	Lake	No	58	430	^{14}C	4E	15.5-0.5	360	Gunin et al., 1999
G18	224	Ugii Nuur Lake	47.77	102.77	1330	Lake	No	2456	2796	^{14}C	2C	9-0	85	Wang et al., 2011
G18	66	Dood Nur Lake	51.33	99.38	1538	Lake	No	6400	4514	^{14}C	2E	14-0	740	Gunin et al., 1999
G18	106	Hovsgol Lake	51.10	100.50	1645	Lake	Yes	276000	29640	^{14}C	5E	12-2.5	190	Prokopenko et al., 2007
G18	276	Khuisiin Lake	46.60	101.80	2270	Lake	Yes	4	118	^{14}C+Pb/Cs	6E	1.2-0	17	Tian et al., 2013
G18	41	Daba Nur Lake	48.20	98.79	2465	Lake	No	157	707	^{14}C	5E	13-0	520	Gunin et al., 1999
G19	328	Bolshoe Eravnoe Lake	52.58	111.67	947	Lake	Yes	9503	5500	^{14}C	3E	7.3-0.2	710	Vipper, 2010
G20	10	Baikel Lake	52.08	105.87	130	Lake	No	3150000	100134	^{14}C	12A	22-0	370	Demske et al., 2005

G20	296	Baikal Lake-CON01-603-5	53.95	108.91	446	Lake	Yes	3150000	100134	^{14}C	10D	15.8-0	270	Demske et al., 2005
G20	135	Lake Kotokel_2010	52.78	108.12	458	Lake	Yes	6900	4687	^{14}C	11E	47-0	220	Bezrukova et al., 2010
G20	134	Lake Kotokel_2009	52.78	108.12	458	Lake	Yes	6900	4687	^{14}C	3E	15-0	500	Tarasov et al., 2009
G20	310	Chernoe Lake	50.95	106.63	500	Lake	Yes	-	250	^{14}C	4E	7-0.7	620	Vipper, 2010
G20	297	Baikal Lake-CON01-605-3	51.59	104.85	675	Lake	Yes	3150000	100134	^{14}C	5D	17.7-0	200	Demske et al., 2005
G20	380	Okunayka	55.52	108.47	802	Bog	Yes	-	-	^{14}C	6C	8.3-2.0	120	Bezrukova et al., 2011
G20	446	Ukta Creek mouth	55.80	109.70	906	Bog	Yes	-	-	^{14}C	3U	5.1-0	160	Bezrukova et al., 2006
G20	450	Cheremushka Bog	52.75	108.08	1500	Bog	Yes	-	-	^{14}C	6C	33.5-0	460	Shichi et al., 2009
G20	298	Baikal Lake-CON01-605-5	51.58	104.85	492	Lake	Yes	3150000	100134	^{14}C	12D	11.5-0	130	Demske et al., 2005
G20	341	Khanda-1	55.44	107.00	867	Bog	Yes	-	-	^{14}C	3C	3.1-0.3	50	Bezrukova et al., 2011
G20	342	Khanda	55.44	107.00	867	Bog	Yes	-	-	^{14}C	6C	5.8-0	140	Bezrukova et al., 2011
G21	275	Qiganhu Lake	42.90	119.30	600	Lake	Yes	190	778	^{14}C	5E	12.1-6.7	35	Hu et al., 2016
G21	232	Wangyanggou	42.07	119.92	751	Lake	No	13	200	^{14}C	1A+3E	5-0	85	Li et al., 2006
G21	230	Wangguantun	40.27	113.67	800	Bog	Yes	-	-	^{14}C	1A+4F	8-3	310	Kong and Du, 1996
G21	6	Anguli Nur Lake	41.33	114.37	1000	Lake	Yes	4264	3684	^{14}C	2U	14-10.5	520	Li et al., 1990
G21	178	Qasq	40.67	111.13	1000	Bog	Yes	-	-	^{14}C	2E	10-0	90	Wang et al., 1997
G21	47	Daihai Lake_2004	40.58	112.67	1220	Lake	Yes	16000	7136	^{14}C	8E	11.5-0	215	Xiao et al., 2004
G21	80	Gaoximage Lake	42.95	115.37	1253	Lake	No	100000	17841	^{14}C	4E	6-0	150	Li C.Y. et al., 2003
G21	95	Haoluku Lake	42.96	116.76	1295	Lake	No	1384	2099	^{14}C	4E	11.5-0	250	Wang et al., 2001
G21	17	Bayanchagan Lake	41.65	115.21	1355	Lake	Yes	636	1423	^{14}C	2B+7E	11.5-0	250	Jiang et al., 2006
G21	144	Liuzhouwan Lake	42.71	116.68	1365	Lake	No	288	957	^{14}C	3E	13-0.5	470	Wang et al., 2001
G21	60	Diaojiaohaizi Lake	41.30	112.35	1800	Lake	Yes	30	309	^{14}C	4U	11.5-2.5	95	Song et al., 1996

G22	112	Hulun Nur Lake_1995	49.28	117.40	544	Lake	No	233900	27286	^{14}C	7U	19-0.5	190	Yang et al., 1995
G22	113	Hulun Nur Lake_2006	49.13	117.51	545	Lake	Yes	233900	27286	^{14}C	13E	11-0	65	Wen et al., 2010
G23	314	Derput	57.03	124.12	700	Bog	Yes	1	56	^{14}C	1A+4C	11.7-0.8	210	Andreev and Klimanov, 1991
G23	409	Suollakh	57.05	123.85	811	Bog	Yes	-	-	^{14}C	8C	12.8-3.7	180	Andreev et al., 1991
G24	379	Nuochaga Lake	61.30	129.55	260	Lake	Yes	120	618	^{14}C	4E	6.5-0	140	Andreev and Klimanov, 1989
G24	307	Chabada Lake	61.98	129.37	290	Lake	Yes	210	818	^{14}C	15U	13-0	110	Andreev and Klimanov, 1989
G25	305	Boguda Lake	63.67	123.25	120	Lake	Yes	2500	2821	^{14}C	7E	10.9-0.4	180	Andreev et al., 1989
G25	344	Khomustakh Lake	63.82	121.62	120	Lake	Yes	440	1183	^{14}C	9E	12.3-0.1	170	Andreev et al., 1989
G25	368	Madjaga Lake	64.83	120.97	160	Lake	Yes	1440	2141	LSC	7E	8.2-0.2	120	Andreev and Klimanov, 1989
G25	302	Billyakh Lake	65.30	126.78	340	Lake	Yes	1678	2311	^{14}C	7A	14.1-0	180	Müller et al., 2009
G25	426	Lake Billyakh_PG1755	65.27	126.75	340	Lake	Yes	1634	2281	^{14}C	1A+10E	50.6-0.2	470	Müller et al., 2010
G26	440	Lake Kyutyunda_PG2022	69.63	123.65	66	Lake	Yes	468	1220	^{14}C	10E	10.8-0.3	360	Biskaborn et al., 2015
G27	435	Khocho	71.05	136.23	6	Bog	Yes	10	178	^{14}C	1C	10.4-0.4	300	Velichko et al., 1994
G27	441	Samandon	70.77	136.25	10	Bog	Yes	100	564	^{14}C	3A+8C+4E	7.9-0.2	280	Velichko et al., 1994
G28	299	Barbarina Tumsa	73.57	123.35	10	Bog	Yes	-	-	^{14}C	4C	4.9-0.3	240	Andreev et al., 2004
G28	373	Lake Nikolay	73.67	124.25	35	Lake	Yes	1500	2185	^{14}C	6A	12.5-0	600	Andreev et al., 2004
G28	318	Dolgoe Ozero	71.87	127.07	12	Lake	Yes	84	517	^{14}C	1A+9B	15.3-0	210	Pisaric et al., 2001
G29	152	Maili	42.87	122.88	155	Bog	No	-	-	^{14}C	5A	3-0	115	Ren and Zhang, 1997
G29	54	Dashan	44.88	124.85	200	Bog	Yes	-	-	^{14}C	5U	7.5-1	160	Xia et al., 1993
G29	240	Xiaonan	43.88	125.22	209	Bog	Yes	-	-	^{14}C	5U	5.5-0	290	Wang and Xia, 1988

G29	197	Shuangyang	43.45	125.75	215	Bog	Yes	-	-	^{14}C	12E	2.5-0	30	Qiu et al., 1981
G29	34	Charisu	42.95	122.35	249	Bog	Yes	-	-	^{14}C	10A	5.5-0	170	Li Y.H. et al., 2003b
G29	463	Jingbo Lake	43.91	128.75	350	Lake	Yes	9500	5499	^{14}C+LSC	3E+4	8.8-0	40	Li et al., 2011
G29	96	Harbaling	43.63	129.20	600	Bog	Yes	-	-	^{14}C	3U	3-0	150	Xia, 1988b
G29	122	Jinchuan	42.35	126.38	620	Bog	Yes	-	-	^{14}C	7A	5.5-0	105	Li Y.H. et al., 2003a
G29	72	Erhailongwan Lake	42.30	126.37	724	Lake	Yes	30	309	^{14}C	2A+14E	22-0	760	Liu Y.Y. et al., 2008
G29	288	Sihailongwan Lake	42.28	126.60	797	Lake	Yes	41	360	^{14}C+varve	40A	16.9-0.2	47	Stebich et al., 2015
G29	94	Hani	42.21	126.52	899	Bog	Yes	1800	2394	^{14}C	1C	9.5-0	455	Qiao, 1993
G29	37	Chichi Lake	42.03	128.13	1800	Bog	Yes	0	40	^{14}C	1C	1-0	140	Xu et al., 1994
G30	21	Belaya Skala	43.25	134.57	4	Bog	Yes	-	-	^{14}C	2A+1C	6.5-3	250	Korotky et al., 1980
G30	36	Chernyii Yar	43.18	134.43	4	Bog	Yes	-	-	^{14}C	4C	10-0.5	260	Korotky et al., 1980
G30	218	Tikhangou	42.83	132.78	4	Bog	Yes	-	-	^{14}C	5U	12-0	500	Korotky et al., 1980
G30	5	Amba River	43.32	131.82	5	Bog	Yes	-	-	^{14}C	1A+1C+1U	5-2.5	300	Korotky et al., 1980
G30	186	Ryazanovka	42.83	131.37	6	Bog	Yes	-	-	^{14}C	7A	6-0.5	540	Shilo, 1987
G30	171	Ovrazhnyii	43.25	134.57	8	Bog	Yes	-	-	^{14}C	3A	7-1	200	Shilo, 1987
G30	175	Peschanka	43.30	132.12	12	Bog	Yes	-	-	^{14}C	3U	22-11	965	Anderson et al., 2002
G30	464	Xingkai Lake	45.21	132.51	69	Lake	Yes	419000	36520	^{14}C+Pb/Cs	3E	28.5-0	150	Ji et al., 2015
G31	220	Tongjiang	47.65	132.50	49	Bog	Yes	-	-	^{14}C	5C	6-0	130	Zhang and Yang, 2002
G31	40	Chuangye	48.33	134.47	50	Bog	Yes	-	-	^{14}C	3U	12-1	400	Xia, 1988a
G31	161	Minzhuqiao	47.53	133.87	52	Bog	Yes	-	-	^{14}C	4U	6.5-0.5	420	Xia, 1988a
G31	180	Qindeli	47.88	133.67	52	Bog	Yes	-	-	^{14}C	1F+7U	13.5-0.5	380	Xia, 1988a
G31	18	Beidawan	48.13	134.70	60	Bog	Yes	8	157	^{14}C	3U	5.5-0.5	350	Xia, 1988a
G31	234	Wuchanghai	47.22	127.33	200	Bog	Yes	-	-	^{14}C	9E	7-0	250	Xia, 1988b
G31	212	Tangbei	48.35	129.67	486	Bog	Yes	-	-	^{14}C	2A	5.5-1	160	Xia, 1996

G32	418	Venyukovka-3	47.12	138.58	5	Bog	Yes	-	-	^{14}C	1A+2C	5.8-3.2	140	Korotky et al., 1980
G32	417	Venyukovka-2	47.03	138.58	6	Bog	Yes	-	-	^{14}C	1A+1C	3.6-0.4	140	Korotky et al., 1980
G32	384	Oumi	48.22	138.40	990	Bog	Yes	-	-	^{14}C	5C	2.6-0.4	80	Anderson et al., 2002
G32	382	Opasnaya River	48.23	138.48	1320	Bog	Yes	-	-	^{14}C	7C	13.3-6.7	360	Korotky et al., 1988
G33	335	Il'inka Terrace	47.97	142.17	3	Bog	Yes	-	-	^{14}C	2C+1F	2.6-1.1	360	Korotky et al., 1997
G33	371	Mereya River	46.62	142.92	4	Bog	Yes	-	-	^{14}C	2C+2F	42.0-0.8	1530	Anderson et al., 2002
G33	401	Sergeevskii	49.23	142.08	6	Bog	Yes	-	-	^{14}C	8A+1C	8.4-2.2	110	Korotky et al., 1997
G34	332	Gurskii Peat	50.07	137.08	15	Bog	Yes	-	-	^{14}C	7C	13.1-1.5	380	Korotky, 1982
G34	453	Gur Bog	50.00	137.05	35	Bog	No	-	-	^{14}C	13C	22.1-0	340	Mokhova et al., 2009
G34	223	Tuqiang	52.23	122.80	400	Bog	Yes	-	-	^{14}C	10A+14E+8F	3-1	125	Xia, 1996
G34	398	Selitkan-2	53.22	135.03	1300	Bog	Yes	-	-	^{14}C	4C	6.4-1.9	260	Volkov and Arkhipov, 1978
G34	397	Selitkan-1	53.22	135.05	1320	Bog	Yes	-	-	^{14}C	6C	7.9-0	140	Korotky et al., 1985
G35	443	Two-Yurts Lake_PG1856-3	56.82	160.04	275	Lake	Yes	1168	1928	^{14}C	5A	6.0-2.8	140	Hoff et al., 2015
G35	444	Two-Yurts Lake_PG1857-2	56.82	160.07	275	Lake	Yes	1168	1928	^{14}C	5A	2.5-0.1	130	Hoff et al., 2015
G35	445	Two-Yurts Lake_PG1857-5	56.82	160.07	275	Lake	Yes	1168	1928	^{14}C	5A	4.4-2.5	120	Hoff et al., 2015
G35	455	Lake Sokoch	53.25	157.75	495	Lake	Yes	41	363	^{14}C	8E	9.7-0.3	250	Dirksen et al., 2012.
G36	330	Glukhoye Lake	59.75	149.92	10	Bog	Yes	-	-	^{14}C	5C	9.4-3.4	1000	Lozhkin et al., 1990
G36	312	Chistoye Lake	59.55	151.83	91	Bog	Yes	-	-	^{14}C	5C	7.0-0	540	Anderson ey al., 1997
G36	363	Lesnoye Lake	59.58	151.87	95	Lake	Yes	13	200	^{14}C	8A	15.5-0	400	Anderson et al., 1997
G36	388	Pepel'noye Lake	59.85	150.62	115	Lake	Yes	0	18	^{14}C	2A	4.3-0	180	Lozhkin et al., 2000
G36	290	Alut Lake	60.14	152.31	480	Lake	Yes	63	448	^{14}C	16A+9B	50.4-0	430	Anderson et al., 1998

G36	391	Podkova Lake	59.96	152.10	660	Lake	Yes	114	602	^{14}C	5A	6.0-0	220	Anderson et al., 1997
G36	370	Maltan River	60.88	151.62	735	Bog	Yes	-	-	^{14}C	4A+7C	12.0-9.4	120	Lozhkin and Glushkova, 1997
G36	411	Taloye Lake	61.02	152.33	750	Lake	Yes	16	227	^{14}C	7A	10.3-0	290	Lozhkin et al., 2000
G36	323	Elikchan 4 Lake	60.75	151.88	810	Lake	Yes	329	1023	^{14}C	16U	55.5-0	440	Lozhkin and Anderson, 1995
G36	331	Goluboye Lake	61.12	152.27	810	Lake	Yes	12	192	^{14}C	11A+2B	9.7-0	240	Lozhkin et al., 2000
G36	470	Julietta Lake	61.34	154.56	880	Lake	Yes	11	189	^{14}C	2A+4E+1I	36.1-1.4	270	Anderson et al., 2010
G36	321	Elgennya Lake	62.08	149.00	1040	Lake	Yes	455	1204	^{14}C	6A	16.0-0	310	Lozhkin et al., 1996
G37	405	Smorodinovoye Lake	64.77	141.12	800	Lake	Yes	27	293	^{14}C	6A+5F	27.1-0	360	Anderson et al., 1998
G37	416	Vechernii River	63.28	147.75	800	Bog	Yes	-	-	^{14}C	1F	14.4-0.1	380	Anderson et al., 2002
G37	338	Jack London Lake	62.17	149.50	820	Lake	Yes	1213	1965	^{14}C	7F	19.5-0.2	320	Lozhkin et al., 1993
G37	406	Sosednee Lake	62.17	149.50	822	Lake	Yes	82	510	^{14}C	4E+1F	26.3-0	640	Lozhkin et al., 1993
G37	393	Rock Island Lake	62.03	149.59	849	Lake	Yes	5	124	^{14}C	2E	6.6-0	470	Lozhkin et al., 1993
G37	381	Oldcamp Lake	62.04	149.59	853	Lake	Yes	7	150	^{14}C	2E	3.7-0	370	Anderson, unpublished
G37	329	Gek Lake	63.52	147.93	969	Lake	Yes	2392	2759	^{14}C	8A+1B	9.6-0	440	Stetsenko, 1998
G37	433	Figurnoye Lake	62.10	149.00	1053	Lake	Yes	439	1182	^{14}C	4A	1.3-0	30	Lozhkin et al., 1996
G38	353	Kuropatoch'ya_Kurop7	70.67	156.75	7	Bog	Yes	-	-	^{14}C	3C	5.7-0.4	760	Anderson et al., 2002
G38	354	Kuropatoch'ya_Kurpeat	69.97	156.38	47	Bog	Yes	-	-	^{14}C	1A+4C	11.7-7.5	430	Lozhkin and Vazhenina, 1987
G39	322	Elgygytgyn Lake	67.50	172.10	496	Lake	No	9503	5500	polarity	-	20.2-1.5	650	Melles et al., 2012
G39	325	Enmynveem_mammoth	68.17	165.93	400	Bog	Yes	50	399	^{14}C	2C+2F	36.4-9.3	2470	Lozhkin et al., 1988
G39	326	Enmyvaam River	67.42	172.08	490	Bog	Yes	18	239	^{14}C	1A+4C	10.6-4.3	630	Lozhkin and Vazhenina, 1987
G39	324	Enmynveem River	68.25	166.00	500	Bog	Yes	-	-	^{14}C	4C	10.7-4.0	420	Anderson et al., 2002

G40	454	Malyi Krechet Lake	64.80	175.53	32	Lake	Yes	125	630	^{14}C	12A	9.6-0	400	Lozhkin and Anderson, 2013
G40	456	Melkoye Lake	64.86	175.23	36	Lake	Yes	1870	2440	^{14}C	21E	39.1-0	1260	Lozhkin and Anderson, 2013
G40	460	Sunset Lake	64.84	175.30	36	Lake	Yes	240	874	^{14}C	7A	14.0-0	260	Lozhkin and Anderson, 2013
G40	333	Gytgykai Lake	63.42	176.57	102	Lake	Yes	99	561	^{14}C	1A+8E	32.3-0	470	Lozhkin et al., 1998
G40	457	Patricia Lake	63.33	176.50	121	Lake	Yes	40	357	^{14}C	3A+7E	19.1-0	290	Anderson and Lozhkin, 2015
G41	436	Konergino	65.90	-178.90	10	Bog	Yes	-	-	^{14}C	1C	9.8-0	900	Ivanov et al., 1984
G41	365	Lorino	65.50	-171.70	12	Bog	Yes	-	-	^{14}C	3C	17.9-5.1	850	Ivanov, 1986
G41	317	Dlinnoye Lake	67.75	-178.83	280	Lake	Yes	71	476	^{14}C	3A	1.3-0	130	Anderson et al., 2002
G41	431	Dikikh Olyenyeii Lake	67.75	-178.83	300	Lake	Yes	64	450	^{14}C	1A+4C	50.3-0	1050	Anderson et al., 2002
G42	427	Blossom Cape	70.68	178.95	6	Bog	Yes	-	-	^{14}C	1C	13.8-0.2	3400	Oganesyan et al., 1993
G42	420	Wrangle Island_Jack London Lake	70.83	-179.75	7	Lake	Yes	69	469	^{14}C	5A+1E	16.1-0.3	790	Lozhkin et al., 2001
G42	419	Wrangel Island	71.17	-179.75	200	Bog	Yes	-	-	^{14}C	17A+3C	13.7-10.2	110	Lozhkin et al., 2001

LSC: liquid-scintillation counting; A: terrestrial plant macrofossil; B: non-terrestrial plant macrofossil; C: peat; D: pollen; U: unknown; E: total organic matter from silt; F: animal remains or shell; G: charcoal; H: $CaCO_3$; I: tephra.

Appendix 3 Slight percentage changes for five major plant taxa reconstructed by REVEALS model with different bog radii (5 m, 10 m, 20 m, 50 m, 100 m, 200 m and 500 m).

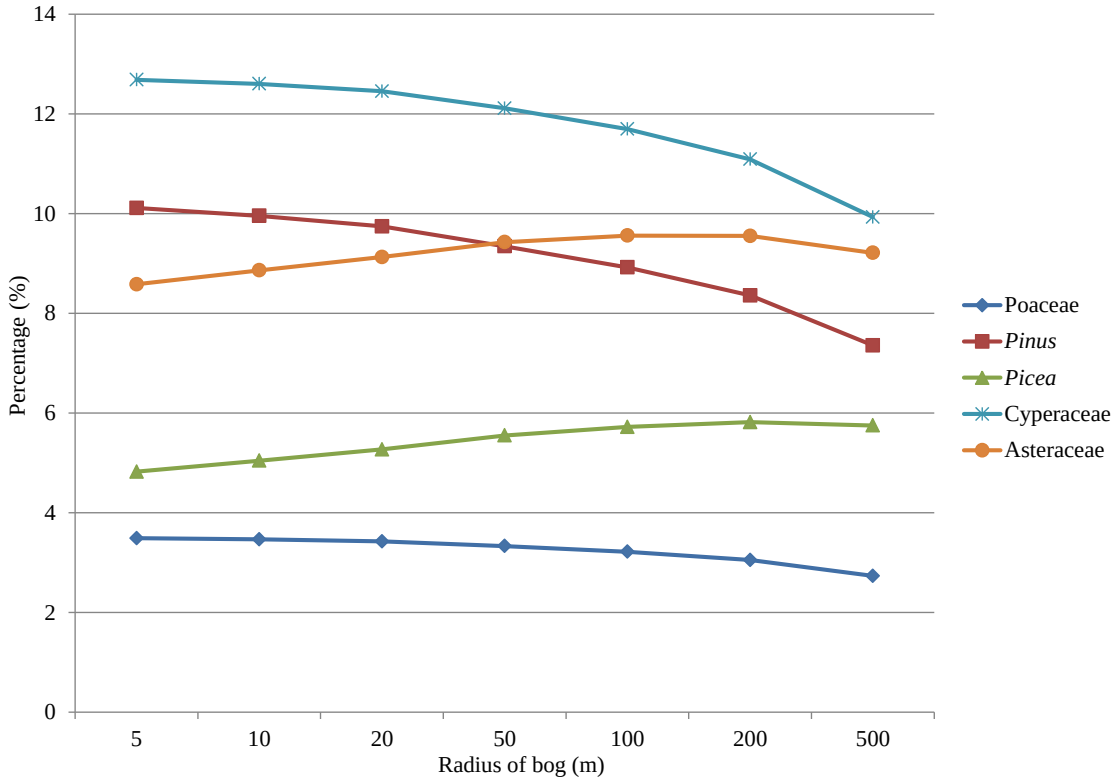

Appendix 4 Pollen Productivity Estimates (PPEs) with their standard errors (SEs) for 27 pollen taxa from 20 study areas. Estimates where SE ⩾ PPE were excluded from the calculation of mean PPE and are shown in italics.

Country	Poland	Russia	Sweden	Sweden	Swiss	Swiss	Switzerland	Sweden	Finland	Estonia
Region	Białowieża Forest	Khatanga region	Southern Sweden	Southern Sweden	Swiss Plateau	Alps	Jura Mountains	west-central	Fennoscandia	Southeast
sample type	Moss	Moss	Moss	Moss	Lake	Trap	Moss	Moss	Moss	Lake
Reference	Baker et al., 2016	Niemeyer et al., 2015	Broström et al., 2004	Sugita et al., 1999	Soepboer et al., 2007	Sjögren et al., 2008	Mazier et al., 2008	von Stedingk et al., 2008	Räsänen et al., 2007	Poska et al., 2011
Model	ERV-3	ERV-2	ERV-3	ERV-3	ERV-3	-	ERV-1	ERV-3	ERV-3	ERV-1
Poaceae	1 (0.00)	1 (0.00)	1 (0.00)	1 (0.00)	1 (0.00)	1 (0.00)	1 (0.00)	1 (0.00)	1 (0.00)	1 (0.00)
Abies					9.92 (2.86)		3.83 (0.37)			
Pinus	23.12 (0.24)			5.66 (0.00)	1.35 (0.45)	9 (0.00)		21.58 (2.87)	8.4 (1.34)	5.07 (0.06)
Picea				1.76 (0.00)	0.57 (0.16)	0.5 (0.00)	7.1 (0.2)	2.78 (0.21)		4.73 (0.13)
Larix		*0.00009 (0.1)*				1.4 (0.00)				
*Alnus*_tree	15.95 (0.66)			4.2 (0.14)		20 (0.00)				13.93 (0.15)
*Betula*_tree	13.94 (0.23)			8.87 (0.13)	2.42 (0.39)			2.24 (0.2)	4.6 (0.7)	1.81 (0.02)
Juglans										
Fraxinus				0.67 (0.03)	1.39 (0.21)					
Quercus	18.47 (0.10)			7.53 (0.08)	2.56 (0.39)					7.39 (0.2)
Tilia	0.98 (0.03)			0.8 (0.03)						
Ulmus										
*Alnus*_shrub		6.42 (0.42)								
*Betula*_shrub		1.8 (0.26)								
Carpinus	4.48 (0.03)				4.56 (0.85)					
Corylus	1.35 (0.05)			1.4 (0.04)	2.58 (0.25)					

Salix	0.03 (0.03)		1.27 (0.31)				0.09 (0.03)			2.31 (0.08)
Ericaceae	0.33 (0.03)						0.07 (0.04)			
Ephedra										
Cyperaceae	0.53 (0.06)	1 (0.16)				0.68 (0.01)	0.89 (0.03)		0.002 (0.0022)	1.23 (0.09)
Artemisia										3.48 (0.19)
Chenopodiaceae										
Asteraceae		0.24 (0.06)		0.17 (0.03)						
Thalictrum										
Ranunculaceae		3.85 (0.72)								
Caryophyllaceae										
Brassicaceae										

1006

Country	Czech	Norway	Greenland	England	England	Germany	China	China	China	China
Region	Central Bohemia	South	Southern	Calthorpe	Wheatfen	Brandenburg	Tibetan Plateau	Xilinhaote	Shandong	Changbai Mt.
sample type	Moss	Lake	Moss	Moss	Moss	Lake	Lake	Soil	moss	Moss
Reference	Abraham and Kozáková, 2012	Hjelle and Sugita, 2012	Bunting et al., 2013	Bunting et al., 2005	Bunting et al., 2005	Matthias et al., 2012	Wang and Herzschuh, 2011	Xu et al., 2014	Li et al., 2017	Li et al., 2015
Model	ERV-1	ERV-3	ERV-1	Average	Average	allFIDage_ERV3	ERV-2	ERV2	ERV-3	-
Poaceae	1 (0.00)	1 (0.00)	1 (0.00)	1 (0.00)	1 (0.00)	1 (0.00)	1 (0.00)	1 (0.00)	1 (0.00)	
Abies										
Pinus	6.17 (0.41)	5.73 (0.07)				5.2 (0.00)			8.96 (0.23)	15.2079 (0.489)
Picea		1.2 (0.04)				1.456 (0.05)				
Larix						8.06 (0.32)				1.47 (0.19)

*Alnus*_tree	2.56 (0.32)	3.22 (0.22)		10.564 (0.00)	4.028 (0.00)	14.248 (0.22)				
*Betula*_tree			3.7 (0.4)	9.804 (0.00)		8.84 (0.34)				24.65 (0.73)
Juglans									0.3 (0.05)	9.49 (0.44)
Fraxinus	1.11 (0.09)			1.14 (0.00)	0.076 (0.00)	6.188 (0.12)				3.72 (0.68)
Quercus	1.76 (0.2)	1.3 (0.1)		7.6 (0.00)	7.6 (0.00)	1.976 (0.03)			4.89 (0.16)	
Tilia	1.36 (0.26)					1.352 (0.04)				0.78 (0.19)
Ulmus								11.5 (1.09)	1 (0.31)	6.85 (1.71)
*Alnus*_shrub										
*Betula*_shrub			1.4 (0.05)							
Carpinus						8.684 (0.09)				
Corylus					1.216 (0.00)					
Salix	1.19 (0.12)	0.62 (0.11)	0.8 (0.002)	1.748 (0.00)	2.736 (0.00)					
Ericaceae										
Ephedra								0.96 (0.14)		
Cyperaceae		1.37 (0.21)	0.95 (0.05)				0.65 (0.4)	0.94 (0.079)	0.21 (0.07)	
Artemisia	2.77 (0.39)						3.2 (0.6)	11.21 (0.31)	24.7 (0.36)	
Chenopodiaceae	4.28 (0.27)						5.3 (1.1)	6.74 (0.79)		
Asteraceae								0.39 (0.16)	1.06 (0.21)	
Thalictrum			4.65 (0.3)					3.06 (0.42)		
Ranunculaceae			1.95 (0.1)							
Caryophyllaceae			0.6 (0.05)							
Brassicaceae								7.48 (0.33)	0.89 (0.18)	

Reference list of Appendix 4:

Abraham, V. and Kozáková, R.: Relative pollen productivity estimates in the modern agricultural landscape of Central Bohemia (Czech Republic). Review of Palaeobotany and Palynology, 179: 1–12, 2012.

1010 Baker, A.G., Zimny, M., Keczyński, N., Bhagwat, S.A., Willis, K.J. and Latałowa, M.: Pollen productivity estimates from old-growth forest strongly differ from
1011 those obtained in cultural landscapes: Evidence from the Białowieża National Park, Poland. The Holocene, 26: 80–92, 2016.
1012 Broström, A., Sugita, S. and Gaillard, M.-J.: Pollen productivity estimates for the reconstruction of past vegetation cover in the cultural landscape of southern
1013 Sweden. The Holocene, 14: 368–381, 2004.
1014 Bunting, M.J., Armitage, R., Binney, H.A. and Waller, M.: Estimates of 'relative pollen productivity' and 'relevant source area of pollen' for major tree taxa in two
1015 Norfolk (UK) woodlands. The Holocene, 15: 459–465, 2005.
1016 Bunting, M.J., Schofield, J.E. and Edwards, K.J.: Estimates of relative pollen productivity (RPP) for selected taxa from southern Greenland: A pragmatic solution.
1017 Review of Palaeobotany and Palynology, 190: 66–74, 2013.
1018 Hjelle, K.L. and Sugita, S.: Estimating pollen productivity and relevant source area of pollen using lake sediments in Norway: How does lake size variation affect
1019 the estimates? The Holocene, 22: 313–324, 2011.
1020 Li, F., Gaillard, M.-J., Sugita, S., Mazier, F., Xu, Q., Zhou, Z., Zhang, Y., Li, Y. and Laffly, D.: Relative pollen productivity estimates for major plant taxa of cultural
1021 landscapes in central eastern China. Vegetation History and Archaeobotany, 26: 587–605, 2017.
1022 Li, Y., Nielsen, A.B., Zhao, X., Shan, L., Wang, S., Wu, J. and Zhou, L.: Pollen production estimates (PPEs) and fall speeds for major tree taxa and relevant source
1023 areas of pollen (RSAP) in Changbai Mountain, northeastern China. Review of Palaeobotany and Palynology, 216: 92–100, 2015.
1024 Matthias, I., Nielsen, A.B. and Giesecke, T.: Evaluating the effect of flowering age and forest structure on pollen productivity estimates. Vegetation History and
1025 Archaeobotany, 21: 471–484, 2012.
1026 Mazier, F., Broström, A., Gaillard, M.-J., Sugita, S., Vittoz, P. and Buttler, A.: Pollen productivity estimates and relevant source area of pollen for selected plant taxa
1027 in a pasture woodland landscape of the Jura Mountains (Switzerland). Vegetation History and Archaeobotany, 17: 479–495, 2008.

1028 Niemeyer, B., Klemm, J., Pestryakova, J.A. and Herzschuh, U.: Relative pollen productivity estimates for common taxa of the northern Siberian Arctic. Review of
1029 Palaeobotany and Palynology, 221: 71–82, 2015.
1030 Poska, A., Meltsov, V., Sugita, S. and Vassiljev, J.: Relative pollen productivity estimates of major anemophilous taxa and relevant source area of pollen in a cultural
1031 landscape of the hemi-boreal forest zone (Estonia). Review of Palaeobotany and Palynology, 167: 30–39, 2011.
1032 Räsänen, S., Suutari, H. and Nielsen, A.B.: A step further towards quantitative reconstruction of past vegetation in Fennoscandian boreal forests: Pollen productivity
1033 estimates for six dominant taxa. Review of Palaeobotany and Palynology, 146: 208–220, 2007.
1034 Sjögren, P., van der Knaap, W.O., Huusko, A. and Leeuwen, J.F.N.: Pollen productivity, dispersal, and correction factors for major tree taxa in the Swiss Alps based
1035 on pollen-trap results. Review of Palaeobotany and Palynology, 152: 200–210, 2008.
1036 Soepboer, W., Sugita, S., Lotter, A.F., van Leeuwen, J.F.N. and van der Knaap, W.O.: Pollen productivity estimates for quantitative reconstruction of vegetation
1037 cover on the Swiss Plateau. The Holocene, 17: 65–77, 2007.
1038 Sugita, S., Gaillard, M.-J. and Broström, A.: Landscape openness and pollen records: a simulation approach. The Holocene, 9: 409–421, 1999.
1039 von Stedingk, H., Fyfe, R.M. and Allard, A.: Pollen productivity estimates from the forest–tundra ecotone in west-central Sweden: implications for vegetation
1040 reconstruction at the limits of the boreal forest. The Holocene, 18: 323–332, 2008.
1041 Wang, Y. and Herzschuh, U.: Reassessment of Holocene vegetation change on the upper Tibetan Plateau using the pollen-based REVEALS model. Review of
1042 Palaeobotany and Palynology, 168: 31–40, 2011.
1043 Xu, Q.H., Cao, X.Y., Tian, F., Zhang, S.R., Li, Y.C., Li, M.Y., Liu, Y.L. and Liang, J.: Relative pollen productivities of typical steppe species in northern China and
1044 their potential in past vegetation reconstruction. Science China: Earth Sciences, 57: 1254–1266, 2014.

Appendix 5 Number of pollen records from large lakes (≥390 m radius; represented by L), small lakes (<390 m radius; represented by S), and bogs (B) for each site-group used to run REVEALS for each time slice. For example, site-group G6 has 2 large lake records, 1 small lake record, and 2 bog records at 4 ka (represented by 2L1S2B).

Grou	0 ka	0.2 ka	0.5 ka	1 ka	2 ka	3 ka	4 ka	5 ka	6 ka	7 ka	8 ka	9 ka	10 ka	11 ka	12 ka	14 ka	21 ka	25 ka	40 ka
G1	1L	1L	1L	-	1L	-	1L	1L	1L	1L	1L	1L	-	-	-	-	-	-	-
G2	6B	1S6B	1S6B	1S6B	1S4B	2S6B	2S6B	1S4B	2S2B	1S	2S	2S	1S2B	1S2B	1S2B	2B	-	-	-
G3	4B	4B	8B	8B	6B	8B	8B	8B	8B	6B	6B	4B	4B	4B	-	-	-	-	-
G4	-	1L	-	1L	1L	1L	1L	1L	1L	1L2B	1L2B	1L	1L	1L	1L	-	-	-	-
G5	4S4B	4S4B	4S4B	4S4B	1S4B	1S4B	1S4B	1S2B	1S2B	1S2B	-	-	-	-	-	-	-	-	-
G6	2L1S2B	1L1S2B	2L1S4B	2L1S4B	2L1S4B	1L1S2B	2L1S2B	1S	1L1S	1L2B	1L2B	1L2B	2B	2B	2B	2B	-	-	-
G7	4B	10B	12B	12B	1L12B	1L12B	1L10B	1L10B	1L10B	1L10B	6B	8B	8B	1L6B	2B	-	2B	-	2B
G8	2B	2B	4B	4B	2B	4B	6B	8B	8B	8B	6B	4B	4B	4B	2B	-	-	-	-
G9	4B	4B	6B	6B	4B	6B	6B	2B	6B	4B	8B	8B	8B	8B	4B	2B	-	-	-
G10	1L	1L	1L	1L	2B	1L2B	1L4B	1L6B	1L8B	1L6B	1L6B	1L6B	1L4B	1L2B	1L	1L	1L	-	-
G11	2L1S	2L1S	2L1S	2L1S	1L1S	2L1S	1L1S	1L1S	2L1S	2L1S	2L	2L	1L	1L	2L	1L	1L	1L	-
G12	6L1S2B	5L1S2B	5L1S2B	6L1S2B	5L1S2B	3L1S2B	5L1S2B	4L1S2B	4L2B	4L2B	5L2B	4L	4L	3L	4L	1L	-	-	-
G13	1L	1L	1L	2L	2L	2L	2L	2L	2L	2L	2L	2L	1L	1L	1L	1L	-	-	-
G14	4L	1L	4L	4L1S	5L1S	5L2S	5L1S	4L1S	3L1S	4L2S	4L2S	4L2S	3L1S	4L2S	4L1S	3L2S	-	-	-
G15	1L	2L	2L	2L	2L	3L	3L	3L	3L	2L	2L	3L	1L	3L	3L	2L	1L	-	-
G16	1L	-	2L	-	2L	2L	2L	1L	1L	2L	2L	2L	2L	2L	3L	1L	2L	3L	-
G17	-	-	-	-	1L	1L	-	1L	1L	1L	1L	1L	-	1L	-	-	-	-	-
G18	2L2S	3L1S	2L2S	4L2S	2L1S	4L1S	5L1S	4L1S	4L1S	4L	5L	4L1S	2L1S	3L1S	4L	2L	-	-	-
G19	-	1L	-	1L	1L	-	1L	1L	-	-	-	-	-	-	-	-	-	-	-
G20	6L6B	4L4B	6L8B	5L1S6B	6L1S8B	5L8B	5L6B	5L1S6B	5L1S6B	5L1S4B	4L4B	4L2B	5L2B	5L2B	6L2B	5L2B	2L2B	2L2B	1L
G21	4L1S2B	2L1S2B	4L1S2B	4L1S2B	3L1S2B	4L2S4B	4L2S4B	3L2S4B	3L1S4B	4L1S2B	5L1S4B	4L1S2B	5L1S2B	6L1S	5L1S	1L	-	-	-
G22	1L	1L	2L	2L	2L	2L	2L	2L	2L	2L	2L	2L	2L	2L	1L	1L	-	-	-
G23	-	-	-	2B	2B	2B	4B	4B	4B	4B	4B	4B	4B	4B	4B	-	-	-	-
G24	2L	2L	2L	2L	2L	2L	2L	2L	2L	1L	1L	1L	1L	1L	1L	-	-	-	-
G25	1L	4L	4L	4L	5L	5L	5L	5L	5L	4L	4L	3L	3L	4L	2L	2L	1L	1L	1L
G26	1L	-	1L	1L	1L	1L	1L	1L	1L	-	-	1L	1L	1L	-	-	-	-	-

G27	-	2B	4B	4B	4B	2B	4B	4B	4B	4B	4B	2B	-	-	-	-	-	-	-
G28	2L	2B	2L2B	1L2B	2L2B	1L2B	2L2B	2B	2L	1L	2L	2L	2L	2L	1L	1L	-	-	-
G29	1L1S10B	1L1S14B	1L2S14B	1L1S16B	1L1S16B	1L2S16B	1L1S10B	1L2S10B	1L1S4B	1L2S4B	1L2S2B	1L1S2B	2S	2S	1S	1S	1S	1S	1S
G30	1L	1L2B	1L6B	1L4B	1L8B	1L8B	1L6B	1L10B	1L8B	1L8B	1L4B	1L4B	1L2B	1L4B	1L4B	1L2B	1L4B	1L4B	4B
G31	2B	2B	10B	14B	12B	14B	10B	12B	10B	4B	2B	4B	2B	4B	4B	-	-	-	-
G32	-	-	4B	4B	4B	2B	2B	2B	2B	2B	2B	2B	2B	2B	-	-	-	-	-
G33	-	-	-	4B	2B	2B	4B	2B	4B	2B	2B	-	-	2B	2B	2B	2B	2B	2B
G34	4B	4B	4B	6B	10B	8B	8B	6B	6B	6B	6B	4B	4B	4B	4B	2B	2B	-	-
G35	-	1L1S	1L1S	1L1S	1L1S	2L1S	1L	1L1S	1L	1S	1S	1S	1S	-	-	-	-	-	-
G36	4L4S2B	2L2S	4L3S	4L4S	4L4S	4L5S	4L4S	3L2S2B	4L2S	2L4S4B	3L4S2B	3L4S	2L4S2B	3L2S2B	2L2S2B	2L2S	2L1S	2L1S	2L1S
G37	3L3S	2L1S2B	3L1S2B	1L3S2B	1L3S2B	2L3S2B	1L3S2B	2L2S2B	3L2S2B	3L1S	1L1S	2L	2L1S	2L1S	1L1S	2L1S	2L1S	1L1S	-
G38	-	-	2B	2B	-	2B	2B	2B	2B	-	2B	2B	2B	2B	2B	-	-	-	-
G39	-	-	-	-	-	1L	1L2B	-	1L4B	2B	1L4B	1L4B	2B	1L4B	1L	1L	1L2B	2B	2B
G40	4L1S	1L	2L1S	3L1S	3L1S	2L	1S	2L	2L1S	1S	1L1S	3L1S	2L	2L	3L	2L	2L1S	1L	1L
G41	2L2B	1L	1L	1L	2B	2B	-	4B	-	4B	4B	4B	2B	1L2B	2B	1L2B	1L	1L	1L
G42	-	1L2B	-	1L	1L	1L	1L	-	-	-	-	-	1L	1L2B	1L4B	1L4B	-	-	-

Appendix 6 Cluster diagram of the site-groups based on the plant functional type dataset

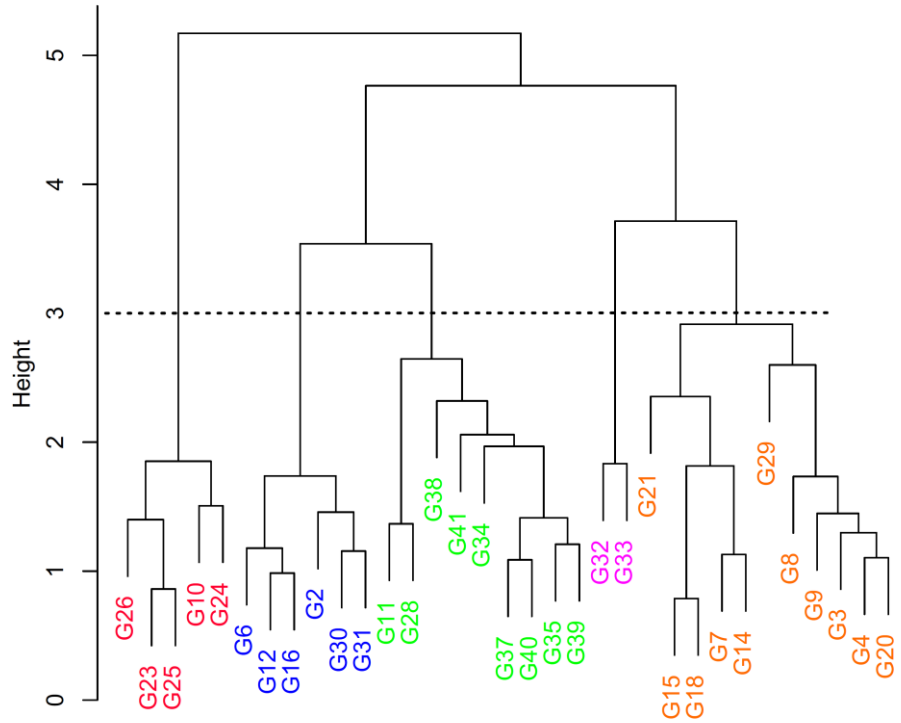

Appendix 7 Map of the study area showing the geographic locations mentioned in the text.

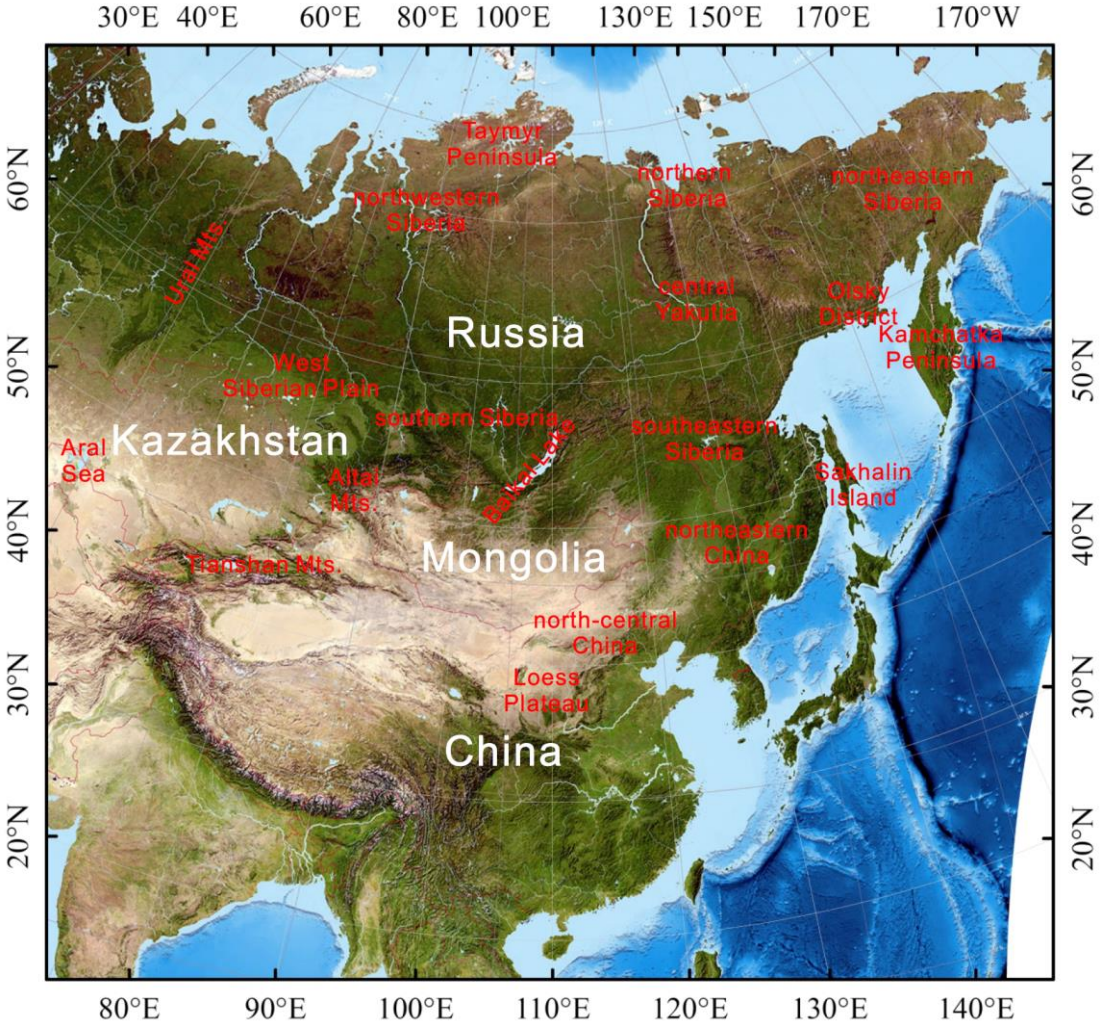

Appendix 8 Selected examples of standard errors for seven plant functional type (PFT) reconstructions at site-groups G21, G20, and G36 at 6 ka.

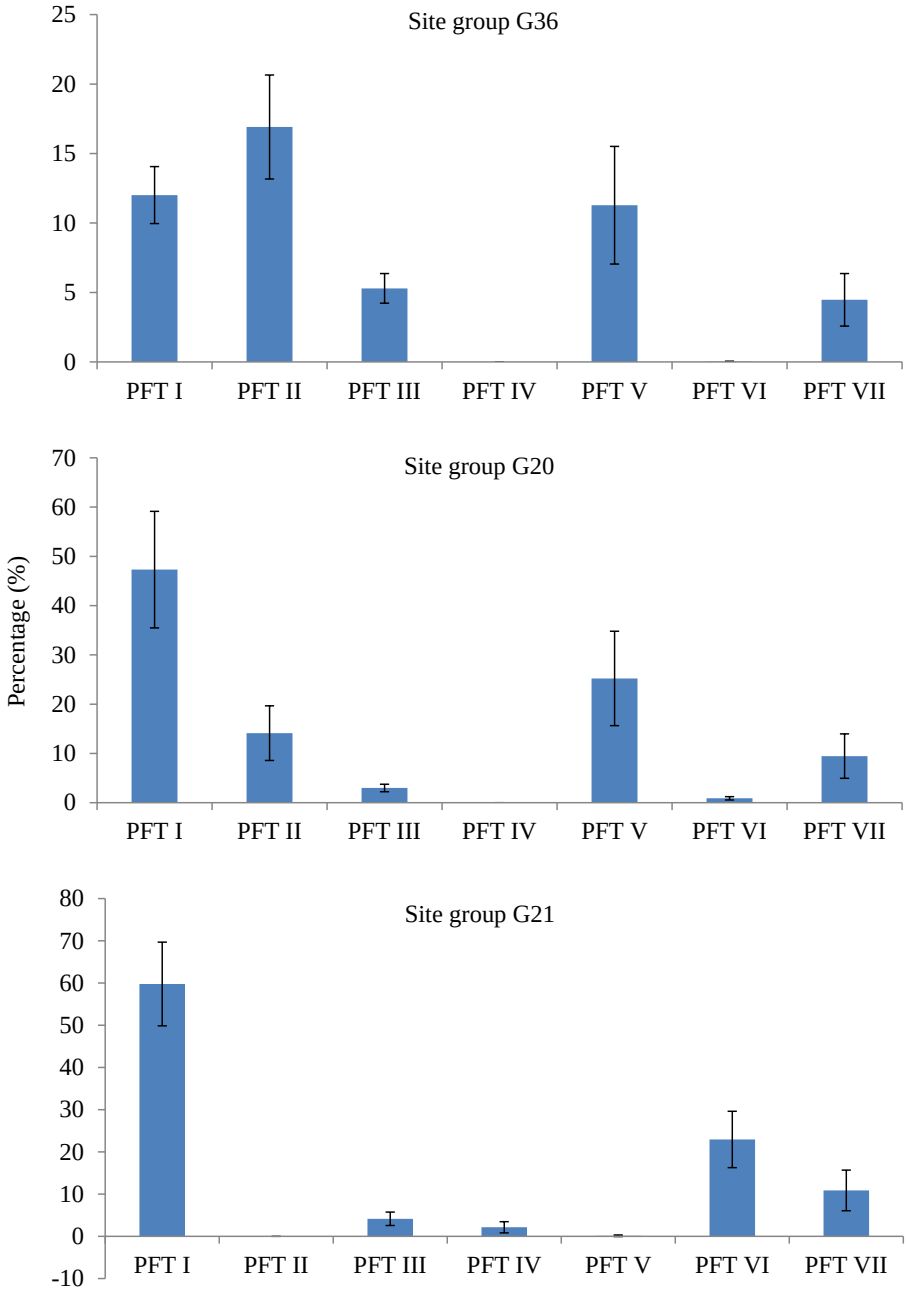

Appendix 9 Proxy-based climate reconstructions from the Northern Hemisphere and insolation variations during the last 40 cal ka BP discussed in the paper. NGRIP: the North Greenland Ice-Core Project (Andersen et al. 2004); Sanbao cave (Cheng et al. 2016); Alkenone-derived sea-surface temperatures (SST) from deep-sea cores SU8118 and MD952042 (Pailler and Bard 2002); solar insolation in July at 60 ºN (Laskar et al. 2004).